Toxicology Reports 9 (2022) 977–998

Contents lists available at ScienceDirect

Toxicology Reports

journal homepage: www.elsevier.com/locate/toxrep

Effect of alpha-mangostin in the prevention of behavioural and neurochemical defects in methylmercury-induced neurotoxicity in experimental rats

Rakesh Sahu [a], Sidharth Mehan [a,*,1,2], Sumit Kumar [a], Aradhana Prajapati [a], Abdulrahman Alshammari [b], Metab Alharbi [b], Mohammed A. Assiri [b], Acharan S. Narula [c]

[a] Neuropharmacology Division, Department of Pharmacology, ISF College of Pharmacy, Moga, Punjab, India
[b] Department of Pharmacology and Toxicology, College of Pharmacy, King Saud University, Post Box 2455, Riyadh 11451, Saudi Arabia
[c] Narula Research, LLC, 107 Boulder Bluff, Chapel Hill, NC 27516, USA

ARTICLE INFO

Handling Editor: Lawrence Lash

Keywords:
Methylmercury
Amyotrophic lateral sclerosis
ERK-1/2
Alpha-mangostin
Oligodendrocytes
Neuroprotection

ABSTRACT

Methylmercury (MeHg+) is a known neurotoxin that causes progressive motor neuron degeneration in the central nervous system. Axonal degeneration, oligodendrocyte degeneration, and myelin basic protein (MBP) deficits are among the neuropathological abnormalities caused by MeHg+ in amyotrophic lateral sclerosis (ALS). This results in demyelination and motor neuron death in both humans and animals. Previous experimental studies have confirmed that overexpression of the extracellular signalling regulated kinase (ERK1/2) signalling contributes to glutamate excitotoxicity, inflammatory response of microglial cells, and oligodendrocyte (OL) dysfunction that promotes myelin loss. Alpha-mangostin (AMG), an active ingredient obtained from the tree "Garcinia mangostana Linn," has been used in experimental animals to treat a variety of brain disorders, including Parkinson's and Huntington's disease memory impairment, Alzheimer's disease, and schizophrenia, including Parkinson's disease and Huntington's disease memory impairment, Alzheimer's disease, and schizophrenia. AMG has traditionally been used as an antioxidant, anti-inflammatory, and neuroprotective agent. Accordingly, we investigated the therapeutic potential of AMG (100 and 200 mg/kg) in experimental rats with methylmercury (MeHg+)-induced neurotoxicity. The neuroprotective effect of AMG on behavioural, cellular, molecular, and other gross pathological changes, such as histopathological alterations in MeHg+ -treated rat brains, is presented. The neurological behaviour of experimental rats was evaluated using a Morris water maze (MWM), open field test (OFT), grip strength test (GST), and force swim test (FST). In addition, we investigate AMG's neuroprotective effect by restoring MBP levels in cerebral spinal fluid and whole rat brain homogenate. The apoptotic, pro-inflammatory, and oxidative stress markers were measured in rat blood plasma samples and brain homogenate. According to the findings of this study, AMG decreases ERK-1/2 levels and modulates neurochemical alterations in rat brains, minimising MeHg+ -induced neurotoxicity.

1. Introduction

Methylmercury (MeHg+) is a mono cationic electrophilic neurotoxin that damages the central nervous system's motor neurons and sensory neurons [1,2]. Long-term exposure to MeHg+ poisoning in different human populations causes distal sensory problems, constriction of visual fields, ataxia, dysarthria, auditory difficulties, and tremors [3].

MeHg+ -induced ALS model causes demyelination and motor neuron death characterised by oligodendrocyte destruction, white matter degeneration, and a decrease in myelin basic protein (MBP) [4,5].

The experimental model of ALS induced by MeHg+ in rats permits researchers to investigate ALS pathophysiological pathways, but it may also open a path for future therapy for ALS patients [6,7]. In-vitro and in-vivo studies show that tissue accumulation of MeHg+ alters the ERK-1/2 signalling pathway [8–10]. Importantly, MeHg+ has been shown to trigger the production of endogenous TDP-43 inclusions [11], which are one of the primary causes of ALS pathogenesis [12]. ALS is a

* Correspondence to: Neuropharmacology Division, Department of Pharmacology, ISF College of Pharmacy, Moga 142001, Punjab, India.
E-mail addresses: sidharthmehan@isfcp.org, sidh.mehan@gmail.com (S. Mehan).
[1] ORCID: https://orcid.org/0000-0003-0034-835X
[2] PUBMED: https://pubmed.ncbi.nlm.nih.gov/?term=Mehan%20 S&sort=pubdate

https://doi.org/10.1016/j.toxrep.2022.04.023
Received 8 April 2022; Received in revised form 17 April 2022; Accepted 20 April 2022
Available online 22 April 2022

Nomenclature

Ach	Acetylcholine
AchE	Acetylcholinesterase
ALS	Amyotrophic lateral sclerosis
AMG	alpha-mangostin
AD	Alzheimer disease
CNS	Central nervous system
CSF	Cerebrospinal fluid
ELISA	Enzyme linked immunosorbent assay
ERK-1/2	Extrcellular signalling regulated kinase-1/2
GABA	Gamma-aminobutyric acid
Glu	Glutamate
GSH	Glutathione
HD	Huntington disease
IL-1beta	Interleukin-1beta
LDH	Lactate dehydrogenase
$MeHg^{+}$	Methylmercury
MBP	Myelin basic protein
MDA	Malondialdehyde
MND	Motor neuron disorder
OL	Oligodendrocyte
PD	Parkinson disease
RT-PCR	Reverse transcription polymerase chain reaction
SOD	Superoxide dismutase
TNF-alpha	Tumour necrosis factor-alpha

neurodegenerative disorder in which motor neurons in the brain cortex, brain stem, and spinal cord gradually die [13–15]. Within 3–5 years, ALS produces muscle weakening and atrophy, which leads to respiratory failure and death. There are two kinds of ALS: sporadic (95%) and familial (5%), both of which are linked to the degradation of cortical and spinal motor neurons [16]. Motor neuron degeneration is a pathological feature of the disease, with loss of both upper and lower motor neurons. MeHg+ -induced ALS complications include progressive limb weakness, respiratory insufficiency, stiffness, hyperreflexia, and bulbar symptoms such as dysarthria, dysphagia, and tongue fasciculations [17]. In ALS patients, mutant proteins such as TDP-43, SOD-1, C9orf-72, and FUS were found in the cytoplasm of diseased neurons [18–20]. A Nature Video, Inside ALS: The neurons behind the disease (See: https://www.youtube.com/watch?v=xrIjFVMliOQ) catches beautifully not only the complexity of this disease but also points to the opportunities that are worthy of pursuit.

The extracellular signal-regulated kinase (ERK-1/2) signalling pathway plays a vital role in the pathogenesis of ALS [21–24]. ERK-1/2 is a critical pathway in the segmentation of oligodendrocytes (OLs) and the synthesis of myelin [25]. Several in-vivo and in-vitro studies have shown that elevated ERK-1/2 expression induces OLs dysfunction, which leads to motor neuron and Schwann cell impairment [26–28].

The ERK-1/2 signalling pathway governs the mitochondria-dependent system and works upstream to stimulate apoptosis in neuronal cells [29]. Activation of ERK-1/2 boosts the inflammatory system by activating glial cells, and it has also been linked to many immunological abnormalities associated with cognition disorders in ALS [30–33].

According to multiple studies, persistent ERK-1/2 signalling pathway overactivation is also reported in many disorders such as Parkinson's disease (PD) [34], Alzheimer's disease (AD) [35], Huntington's disease (HD) [36], cerebral ischaemia [37], cancer, and asthma [38,39]. The expression of ERK-1/2 in astrocytes of SOD1G93A mice has been associated with motor neuron dysfunction (MND) [40]. Furthermore, ERK-1/2 activation results in the generation of neuroinflammatory cytokines such as IL-1β and TNF-α [41,42]. Furthermore, ERK1/2 activation has been connected to glutamate excitotoxicity mediated by microglia and astrocytes [43]. The ERK-1/2 pathway is essential for the future therapy of various disorders, including cancer and NDs [44]. PD98059 and U0126 were the first ERK-1/2 inhibitors used in treating cancer cells [45,46]. The novel ERK-1/2 inhibitors were identified, such as PD0325901 [47], selumetinib [48], and erlotinib [49], for the treatment of neurological disease. Trametinib's ability to downregulate the ERK-1/2 signalling pathway as a therapeutic therapy for ALS has been investigated at the Phase I level (https://clinicaltrials.gov/ct2/show/NCT04326283). USFDA approved the two drugs, riluzole, and edaravone, for the symptomatic treatment of ALS. Riluzole protects neuronal cells from glutamate excitotoxicity by inhibiting glutamate receptors [50,51]. Edaravone has been developed as a potential ROS scavenger [52,53]. Several novel therapeutic approaches are being explored, leading to more successful treatment in the coming days. Alpha-mangostin (AMG) is a xanthone isolated from the pericarp berries and bark of the mangostin tree (Garcinia mangostana Linn.), also known as "the queen of berries". The AMG has neuroprotective [54], anti-oxidant [55], anti-inflammatory [56], and antibacterial properties [57]. AMG inhibits the overactivation of the ERK-1/2 signalling pathway [58]. It has been shown to have protective effects in the treatment of Alzheimer's disease [59], Parkinson's disease [54], Huntington's disease [60], memory impairment [61], and schizophrenia [62].

The ERK-1/2 signalling pathway is active in multiple biological activities, including cell proliferation, gene expression, locomotion, development, and cellular damage [39,63]. Recent research has linked alterations in the ERK-1/2 signalling pathway to the development of ALS and related neuro-complications.This study investigates the neuroprotective effects of AMG on several biological samples, including rat blood plasma, brain homogenate, and CSF. The suppression of ERK-1/2 signalling by AMG may reduce and delay the development of the ALS condition, acting as a preventive treatment against ALS. Based on the above, the MeHg+ model was utilised to develop ALS in rats. It shows motor and behaviour impairment, dysregulation of cellular and molecular pathways, neuronal death, and alterations. The current study investigated the neuroprotective effects of AMG as an ERK-1/2 inhibitor in rats treated with MeHg+.

2. Materials and methods

2.1. Experimental animals

A total of 36 animals were used in this study. Six groups of animals were randomly assigned (n = 6 for each sex group). Adult Wistar rats aged six months and weighing an average of 250–300 g were obtained from the Central Animal House of the ISF College of Pharmacy in Moga, Punjab, India. The animals were housed in an acclimatised room maintained at a 22–25 °C with a 12-hour light/dark cycle and free access to food and water. The Institute for Animal Ethics Committee (IAEC), ISF College of Pharmacy, Moga, Punjab, India, approved project 816/PO/ReBiBt/S/04/CPCSEA as IAEC/CPCSEA/M 28/2020/Protocol No.464, following the guidelines provided by the government of India. The study is reported following ARRIVE guidelines. Animals were acclimatized to laboratory conditions before experimentation.

2.2. Drugs and chemicals

MeHgCl was purchased from Sigma–Aldrich (St. Louis, MI, USA). BAPEX, New Delhi, India, provided an ex-gratia sample of AMG. All of the other chemicals used in the experiment were of analytical grade. The drug and chemical solutions were freshly prepared before use. AMG

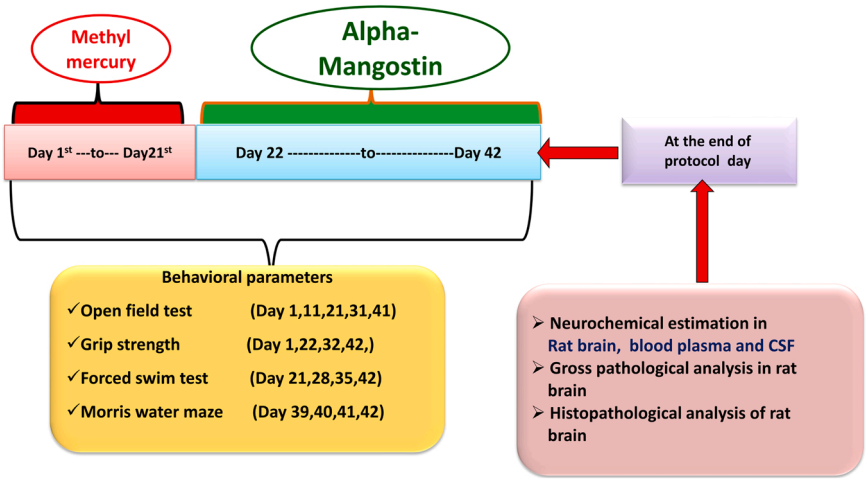

Fig. 1. Experimental protocol schedule.

dissolved in 0.1% CMC and administered orally [58].

2.3. Protocol schedule of animal experimentation

The study lasted a total of 42 days from start to finish. MeHg+ was administered orally from the first to the twenty-first day. From the 21st day of the experiment until the end of the schedule, AMG is administered continuously. The experiment was not blinded, and the researchers were well-known in terms of animal care. From the first through the 42nd day, various behavioural assessments were performed. The 36 animals were divided into six groups each at randomly. Group 1 normal control, Group 2 vehicle control(0.1% CMC from day 22 to day 42), Group 3 AMG200 perse (from day 22 to day 42), Group 4 MeHg+ (from day 1 to day 21), Group 5 MeHg+ (from day 1 to day 21)+ AMG100 (from day 22 to day 42), Group 6 MeHg+ (from day 1 to day 21)+ AMG200 (from day 22 to day 42). Behavioural parameters such as the open field test (OFT), Morris water maze (MWM), and forced swim test (FST) were performed on specific days. On day 43rd, animals were deeply anaesthetised with sodium pentobarbital (270 mg/ml, i.p.) and transcardially perfused with ice-cold PBS (0.1 M) for biochemical, inflammatory, and neurochemical analysis of the rat's brain. The protocol for the experiment is summarised in (Fig. 1).

2.4. MeHg+ -induced experimental model of ALS

According to our laboratory findings, we successfully developed an animal model of MeHg+ -induced ALS-like neurobehavioural and neurochemical changes in adult wistar rats. The adult Wistar Rats were given MeHg+ via oral gavage at a dose of 5 mg/kg daily for 21 days. According to our laboratory previous research, MeHg+, a potent neurotoxin capable of rapidly permeating neural tissue, was shown to be identical to ALS signs and symptoms, as well as neurochemical changes [5–7]. As a result, MeHg+ was employed to study behavioural and neurochemical alterations in rats in this research.

2.5. Parameters assessed

2.5.1. Measurement of weight variations

2.5.1.1. Measurement of body weight. The rats were weighed on the 1st, 7th, 14th, 21st, 28th, 35th, and 42nd days using a standard digital balance. The animals were usually weighed between 10:30 a.m. and 1 p.m. to eliminate diurnal variations [64].

2.5.1.2. Measurement of ratio of brain/body weight. The brain/body weight ratios were measured at the end of the experimental protocol to evaluate the relationship between brain weight and body weight. The rats' heads were removed from their bodies through an incision behind the occipital bone [65]. At the foramen magnum, the brain was separated from the spinal cord. The rats' skulls were carefully removed, and the brains were extracted following this procedure; the fresh brain was weighed without the olfactory bulb.

2.5.2. Behavioural parameters

2.5.2.1. Morris water maze task. Animal's spatial learning and memory were examined in a Morris water maze on the protocol schedule's 39th, 40th, 41st, and 42nd days. It was composed of a circular water tank (180 cm diameter, 60 cm height) filled to a depth of 40 cm with water (25 ± 1 °C) (Siddiqui et al. [145]). A non-toxic water-dispersible emulsion was utilised to make the water opaque. Starting points were chosen at four evenly spaced spots around the pool's edge (North, South, East, and West), dividing the pool into four quadrants. A 10-cm-diameter escape platform was placed in the pool, 2 cm below the water's surface. The escape platform was positioned in the middle of one of the pool's randomly selected quadrants and remained in that position throughout the experiment (northeast for this study).

Before the training began, the rats were permitted to swim freely in the pool for 120 s without a platform. Each trial had a ceiling time of 120 s and a trial interval of approximately 120 s. Animals received a training session consisting of 4 trials per session (once from each starting point) for four days (day 1, 2, 3, and 4) before the final trial, i.e., on the 39th, 40th, 41st 42nd day according to the protocol schedule. The animals remained on the hidden platform for 30 s after climbing onto it before moving on to the next trial. If the rat did not find the hidden platform within the maximum duration of 120 s, it was gently placed on it and permitted to stay there for the same time. TSTQ (time spent in the target quadrant zone) was also measured in order to find the hidden platform. A probing test (day 42nd) was performed 24 h following the acquisition phase by removing the platform. Rats were permitted to swim freely in the pool for 120 s, during which time the time spent in the target quadrant, which previously housed the hidden platform, was recorded. The time spent in the target quadrant showed the degree of memory consolidation following learning [66–68].

2.5.2.2. Grip strength test. The grip strength test examines neuromuscular activity, measured as maximum muscle strength in the forelimbs and combined forelimbs and hind limbs. The apparatus consisted of a metal bar connected to a force transducer. The rats evaluate these by gripping a grid-connected to a sensor. Rats are kept on the tail and

observed to the unit Kgf before gripping a handle on both sides. Rats were pulled back gently until they let go of the handle. Grip intensity was checked four times during the protocol schedule on the 1st, 22nd, 32nd, and 42nd days [69].

2.5.2.3. Forced swim test. The FST is the most common preclinical method for assessing antidepressant operation. Due to its simplicity, consistency across laboratories, and ability to detect a wide range of antidepressant agents, this assay is widely used as a model of antidepressant activity. The immobility time was recorded on the 21st, 28th, 35th, and 42nd treatment days. Each animal was examined in the cylinder for five minutes. The time spent by the rat making only minor motions to keep its heads above water level and the latency to float and floating durations were all recorded. Rats were forced to swim in an unavoidable condition during the forced swim experiment. After a prolonged attempt, the animal becomes immobile or just moves to keep his head above water, and this test's immobility suggests a state of despair [70,71].

2.5.2.4. Open field test. An OFT is an experimental test designed to evaluate the locomotor activity and anxiety-like behaviour. After preparing the apparatus, a single rat was placed at the centre of the area; time was immediately started, and exploratory activity was allowed for 5 min. The silence was maintained throughout the testing process. Following the completion of the test, the rat was returned to its cage. Rats have observed crossing lines (the number of crossed segments with four paws) and rearing for five minutes, and the locomotive activity indicator was used. The open-field test was repeated five times on the 1st, 11th, 21st, 31st, and 41st days of treatment [6].

2.5.3. Neurochemical parameters

2.5.3.1. Collection and preparation of biological samples. Adult Wistar rats' cerebrospinal fluid (CSF) and blood plasma were collected on day 43 [71]. The experiment was carried out to evaluate neurochemicals, antioxidants, apoptotic and molecular markers. First, animals were anaesthetised with sodium pentobarbital (270 mg/ml, i.p.), then, 2.5 ml of blood was collected from anaesthetised rats through retro-bulbar puncture from the orbital venous plexus and a capillary tube inserted medially into the rat's eye. Blood from the plexus was collected using capillary action through gentle rotation and retraction of the tube into a sterile eppendorf tube containing EDTA. The plasma was separated from freshly collected blood samples by centrifugation at 10,000g for 15 min, and the supernatant was carefully preserved in a deep freeze (at −80 °C) for future use.

Before the CSF collection, the fur on the rat's neck area was removed with an Oster clipper. After that, the anaesthetised rat was mounted in a stereotaxic frame and supported with ear bars. The animal's head was held at a 45° angle downward. A needle attached to a syringe was inserted horizontally and centrally into the cisterna magna [72]. Approximately 100–150 μL of CSF sample was slowly drawn into the syringe [73,74]. To evaluate cellular markers and MBP, the sample was stored at − 80 °C until the experiments.

Animals were decapitated immediately after blood and CSF collection, and the brains were collected with ice-cold PBS (0.1 M) followed by PBS for biochemical analysis of the brain. Individual fresh brains were weighed before gross pathology and brain sectioning. The brain tissue was placed in a 3–4 vol cold homogenisation buffer per tissue volume, and the mixture was transferred to the homogeniser. Using a mechanical shear homogeniser, homogenise the tissue 3–4 times for 20–30 s each, pausing for 10–15 s between each homogenisation. Cell debris and other particulate matter were removed from the homogenate by centrifugation at 10,000 g for 10–20 min at 4 °C, and the homogenate was preserved at − 80 °C until the experiments [75].

2.5.4. Measurement of cellular and biochemical marker

2.5.4.1. Estimation of ERK-1/2 levels. The ERK-1/2 levels are determined using ELISA commercial kits (E-EL-H1698; Elabsciences, Wuhan, Hubei, China). This test was performed according to the standard procedure on CSF samples and rat brain homogenate. The values are expressed as pg/ml protein [58,76].

2.5.4.2. Estimation of myelin basic protein (MBP) levels. ELISA commercial kits (E-EL-R0642/MBP; Elabsciences, Wuhan, Hubei, China) measure myelin basic protein concentration. This test was performed on the brain homogenate and Cerebrospinal fluid (CSF) as per the given standard procedure. The values are expressed as μg/mg protein in brain homogenate and μg/L in the CSF sample [6].

2.5.4.3. Assessment of caspase-3, Bcl-2, and bax levels. Apoptotic markers such as caspase-3 [77,78], Bax [79], and Bcl-2 [80] were evaluated following instructions provided by ELISA test kits (E-EL-R0160/Caspase-3; E-EL-R0098/Bax/Bcl2Elabsciences, Wuhan, Hubei, China) in homogenate and blood plasma.

2.5.5. Neurotransmitter's evaluation

2.5.5.1. Measurement of glutamate and GABA levels. The quantitative analysis of the tissue samples was carried out according to Rajdev et al. Glutamates and gamma-aminobutyric acid (GABA) [81] were quantified after derivation with OPA/β-ME (o-phthaldihyde/β-mercaptoethanol). The neurotransmitter values were expressed as ng/mg protein in brain homogenate [82].

2.5.5.2. Estimation of acetylcholine (Ach) levels. A kit for detecting acetylcholine was used (E-EL-R0355; ELabSciences, Wuhan, Hubei, China). Samples and all reagents were produced following the kit's instructions. The optical density of the reaction mix was evaluated in the microtiter plate at 540 nm. The neurotransmitter concentration in the supernatant was measured in nanograms per milligram of protein [58,83].

2.5.5.3. Measurement of serotonin levels. Using high-performance liquid chromatography (HPLC), the concentration of serotonin in tissue homogenate was determined. A pH-acetonitrile sodium citrate buffer was used in this movement phase (pH4.5). The buffer contained 10 mmol/l citric acid, 25 mmol/l NaH2HPO4, 25 mmol/l EDTA, and 2 mmol/l sulphonic acid one heptane. The experimental electrochemical conditions varied from 5 to 50 nA and were + 0.75 V. Separation was performed at a flow rate of 0.8 ml/min. 20 l of samples were injected manually. Brain samples were normalised to 0.2 mol/l perchloric acid on the experiment day. The samples were then centrifuged at 12,000 g for five minutes. The standard curve has been used to determine the standard serotonin concentrations in the range of 10–100 mg/ml [80,84].

2.5.6. Evaluation of neuroinflammatory cytokines

2.5.6.1. Assessment of TNF-α and IL-1β levels. To determine the quantity of TNF-α [11] and IL-1β [7], a rat tumour necrosis factor- (TNF- α) and interleukin-1 (IL-1β) immunoassay kit was utilised (E-EL-R0019/TNF-α; E-EL-R0012/IL-1β; ELabSciences, Wuhan, Hubei, China). IL-1β and TNF-α are expressed as pg/mg proteins in rat blood plasma and brain homogenate.

2.5.7. Evaluation of oxidative stress markers

2.5.7.1. Measurement of acetylcholinesterase (AchE) levels. Quantitative measurements of AchE activity in brain homogenate were made using

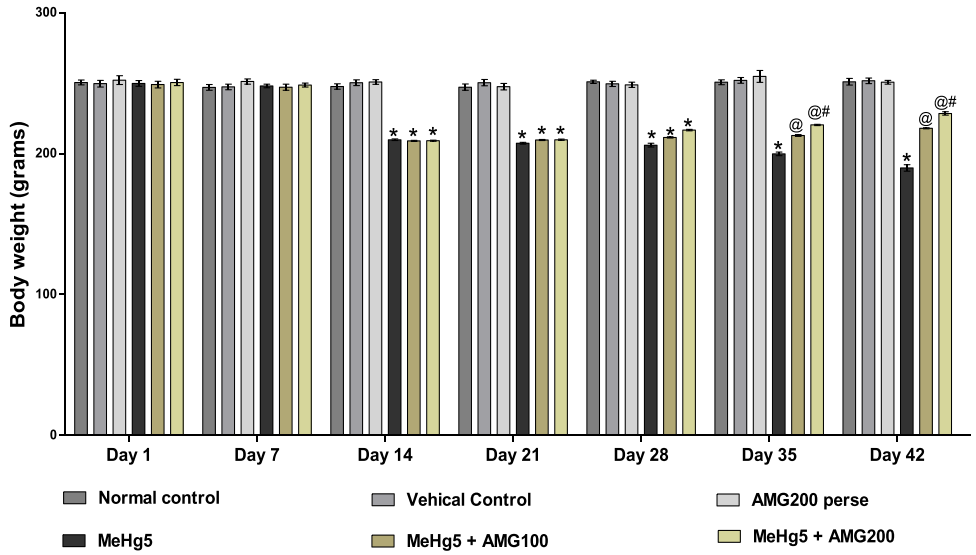

Fig. 2. Effect of α-mangostin on body weight in methylmercury-induced neurotoxicity in experimental rats. Statistical analysis followed by two-way ANOVA (post-hoc Bonferroni's test), * $p < 0.001$ v/s normal control; vehicle control and AMG200 perse; @ $p < 0.001$ v/s MeHg5; @ # $p < 0.001$ v/s MeHg5 +AMG100; ($n = 6$ rats per group).

the method described in this paper [85]. The test mixture contains 0.15 ml of supernatant, 0.01 M sodium phosphate buffer (pH = 8), 0.10 ml of acetyl thiocholine iodide, and 0.10 ml of DTNB (Ellman reagent). The absorbance change was recorded immediately at 412 nm spectrophotometrically.

2.5.7.2. Assessment of reduced glutathione levels. The concentration of GSH in brain homogenate was determined. This method applies to all acid-soluble thiols; glutathione accounts for more than 90% of reactive thiol groups. The assay is based on reducing 5,5'-dithiobis-(2-nitrobenzoic acid)(DTNB) in water at neutral and alkaline pH by glutathione SH groups, which ionise to NTB2-dianion 9 yellow colour. NTB2 was quantified using a spectrophotometer, and its absorbance at 450 nm was represented as mol/g wet tissue. 0.1 M potassium phosphate pH8.4 (5.225 g K2HPO4 in 100 ml DDW, pH 8.4, adjusted with 1 N HCl), DTNB (0.002%) (2 mg/100 ml of 1% sodium citrate solution), and reduced glutathione were used in the estimation process. To prepare the standard graph, reduced glutathione was used as the reference standard. To 2 ml of 0.1 M potassium phosphate pH8.4, 0.1 ml of standard or experimental sample (deproteinized with 10% TCA), 0.5 ml of DTNB, and 3 ml of double distilled water were added. After 10 min at room temperature, the mixture was measured for absorbance at 45 nm, and the GSH content was calculated using a standard graph. Glutathione is expressed as a U/mg protein in the tissue homogenate [86].

2.5.7.3. Estimation of malondialdehyde (MDA) levels. The level of MDA in tissue homogenates was evaluated as a measure of lipid peroxidation. Malondialdehyde (MDA) is one of several low molecular weight end products of the decomposition of lipid hydroperoxides and is the most commonly used indicator of lipid peroxidation. At pH3.5, one molecule of malondialdehyde interacts with two molecules of 2-thiobarbituric acid (TBA) to create a pink chromagen that is spectrophotometrically detected at 532 nm with an extinction coefficient of 156 mM^{-1} cm^{-1}. The estimation was performed using 8.1% SLS (sodium lauryl sulphate),

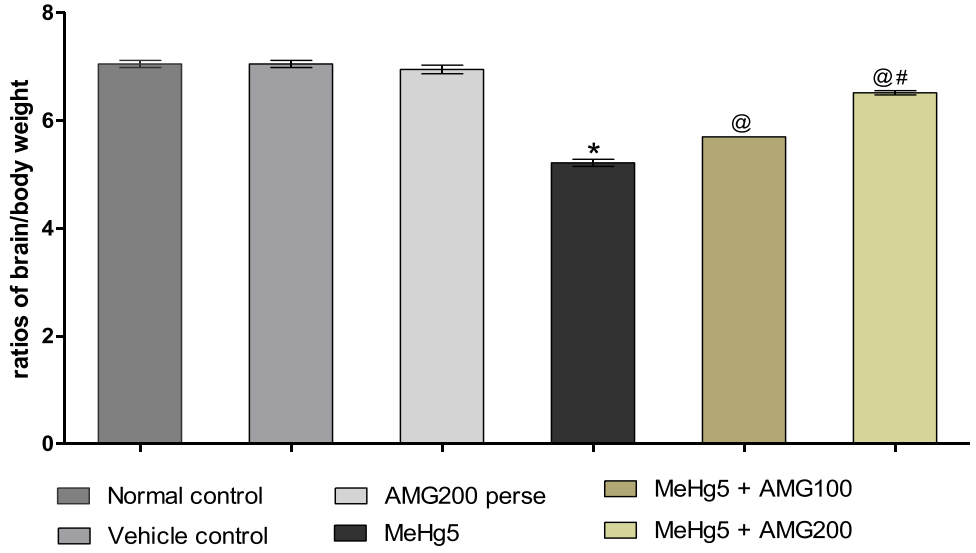

Fig. 3. Neuroprotective effect of α-mangostin on relative brain/body weight ratios in methylmercury-induced neurotoxicity in experimental rats. Statistical analysis followed by one-way ANOVA (post-hoc Tukey's test), * $p < 0.001$ v/s normal control; vehicle control and AMG200 Perse; @ $p < 0.001$ v/s MeHg5; @ # $p < 0.001$ v/s MeHg5 + AMG100; ($n = 6$ rats per group).

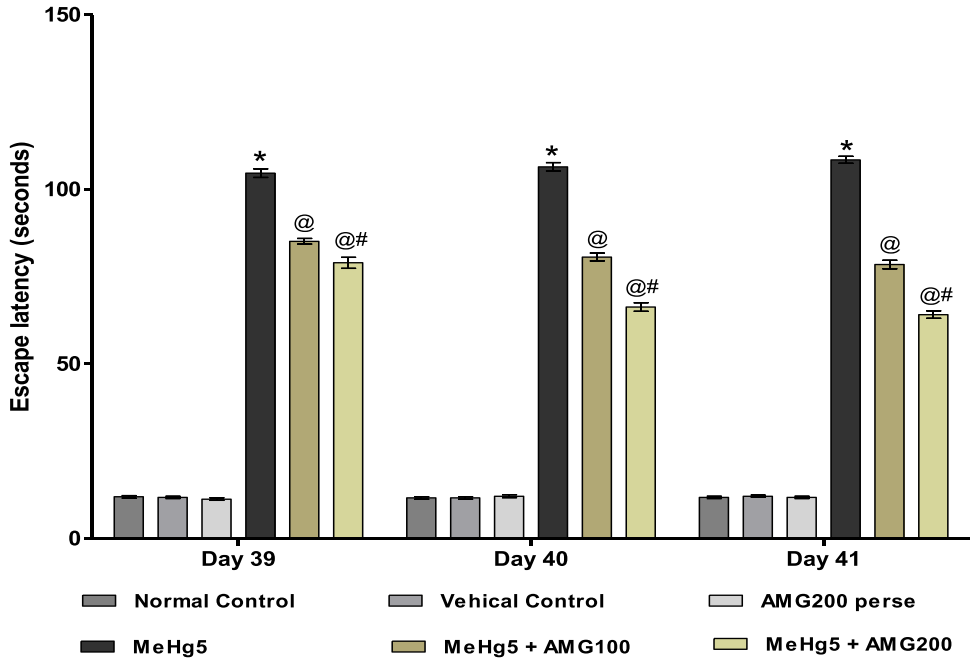

Fig. 4. Neuroprotective effect of α-mangostin on escape latency by using morris water maze task in methylmercury-induced neurotoxicity in experimental rats. Statistical analysis followed by two-way ANOVA (post-hoc Bonferroni's test), * $p < 0.001$ v/s normal control; vehicle control and AMG200 perse; @ $p < 0.001$ v/s MeHg5; @ # $p < 0.001$ v/s MeHg5 +AMG100; (n = 6 rats per group).

20% acetic acid (9.5 ml glacial acetic acid diluted to 50 ml with DDW (pH3.5 with 4 N NaOH), and 0.8% aqueous solution of TBA (2-thiobarbituric acid). All reagents were freshly prepared, and 0.2 ml of 8.1% SLS, 1.5 ml of 20% acetic acid (pH3.5), and 1.5 ml of 0.8% aqueous solution of TBA were added to the 0.2 ml of the experimental sample. The volume was increased to 4 ml with double distilled water. Then, in a water bath over a hotplate, heat the mixture to 95 °C for 60 min to generate a light pink colour. Allowing the mixture to cool, the absorbance at 532 nm was measured spectrophotometrically using a microplate reader (Biotek Instruments, Synergy 4, USA). The MDA content was calculated using an extinction coefficient of 156 mM^{-1} cm^{-1} and expressed as nmol/g wet tissue. Finally, the MDA content was determined using the following formula. Lipid peroxides (nmol MDA/g brain tissue) = (abs/156) × [total volume (4 ml)/ sample volume (0.2 ml)] × dilution factor (10) × 1000). The MDA concentration was quantified as U/mg protein [87].

2.5.7.4. Measurement of superoxide dismutase (SOD) levels. The superoxide dismutase (SOD) Assay kit manufactured by Sigma-Aldrich was utilised for the quantitative in vitro determination of Superoxide dismutase (SOD) in brain tissue. The approach utilised is the colorimetric method. SOD assaying by a highly water-soluble tetrazolium salt, WST-1 (2-(4-Iodophenyl) - 3-(4- nitro phenyl)– 5-(2, 4-disulfophenyl)- 2H-tetrazolium, monosodium salt) that produces a water-soluble formazan dye upon reduction with a superoxide anion. The rate of the decrease with O2 is linearly related to the xanthine oxidase (XO) activity and is hindered by SOD, as demonstrated in Fig. 4. Therefore, a colourimetric approach can evaluate the IC50 (50% inhibitory activity of SOD or SOD-like compounds). The absorbance at 440 nm is proportional to the amount of superoxide anion. The SOD activity as an inhibitory activity can be assessed by measuring the decrease in colour development at 440 nm. The amount of SOD is expressed in units per milligram of protein (U/mg) [88,89].

2.5.7.5. Estimation of nitrite levels. The accumulation of nitrite in the supernatant, an indicator of nitric oxide (NO) production, was measured using a colorimetric assay with Greiss reagent [0.1% N-(1-naphthyl) ethylenediamine dihydrochloride, 1% sulphanialamide, and 2.5% phosphoric acid]. After mixing equal volumes of supernatant and Greiss reagent, the mixture was incubated for 10 min at room temperature in the dark. The absorbance at 540 nm was measured using Perkin Elmer Lambda 20 spectrophotometers. The nitrite concentration in the supernatant was calculated using a sodium nitrite standard curve and expressed as a percentage of the control. The concentration of nitrite in the homogenate of the brain is expressed as mM/mg protein [90].

2.5.7.6. Estimation of lactate dehydrogenase (LDH) levels. The level of LDH was measured using UV spectrophotometric. LDH catalysers lactate oxidation while reducing nicotinamide adenine dinucleotide (NAD) to NADH [91]. The concentration of LDH is expressed as a U/mg in brain homogenate. In supernatant, a lactate dehydrogenase detection kit (Coral Diagnostics, Indian) was used to detect LDH levels [82].

2.5.7.7. Estimation protein level. The Coral protein estimation kit was used to determine the protein content (Biurette method). The reagent is used in the biuret protein assay, a colorimetric test that measures protein content in rat brain homogenate using UV/visible spectroscopy at 540 nm.

2.5.8. Assessment of gross pathology and morphology

On day 43, the animals were decapitated, and their brains were taken for gross pathological examination. After examining the entire rat brain, coronal slices were prepared. On glass slides, 2-mm thick sectioned brain sections were placed [80]. All brain components were photographed with a digital camera (Fujix digital camera, Fujifilm, Japan). The demyelination region (mm) of each brain segment was measured using MOTICAM-BA310 image plus 2.0 analysis software on the 43rd day of the procedure. The conversion of the demyelination region for each segment of the coronal brain produced the demyelination volume (mm3) [92,93]. On the 43rd day, an imaging evaluation was performed to determine each brain region's demyelination (mm3) size. The damage size was determined by estimating the demyelination area in each 2 mm thick coronal brain segment [77].

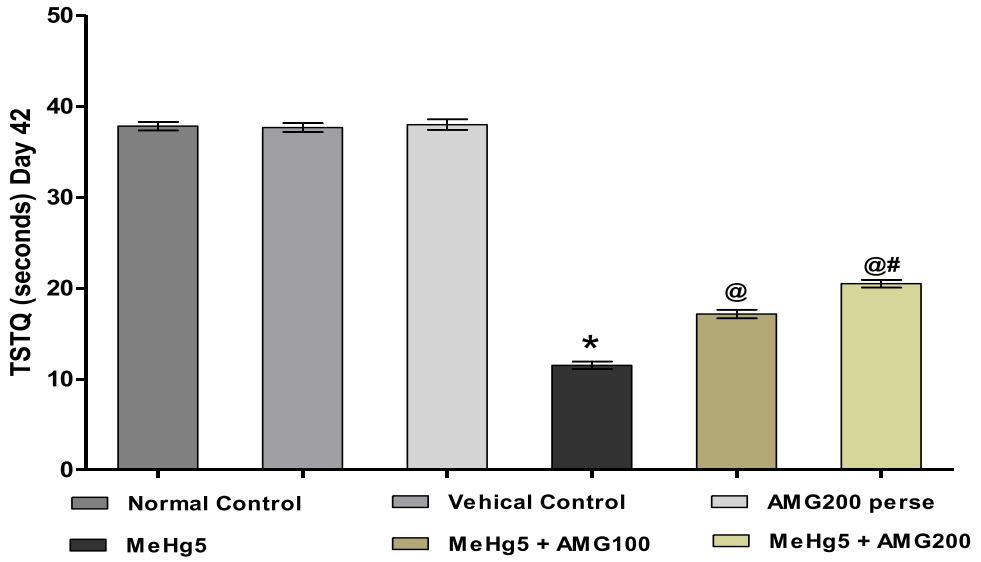

Fig. 5. Neuroprotective effect of α-mangostin on time spent in the target quadrant (TSTQ) using morris water maze in methylmercury-induced neurotoxicity in experimental rats. Statistical analysis followed by one-way ANOVA (post-hoc Tukey's test), * $p < 0.001$ v/s normal control; vehicle control and AMG200 Perse; @ $p < 0.001$ v/s MeHg5; @ # $p < 0.001$ v/s MeHg5 + AMG100; ($n = 6$ rats per group).

2.5.9. Assessment of histopathological changes

After the experimental regimen was completed, the animals were completely anaesthetised with sodium phenobarbital (270 mg/ml, i.p.) and sacrificed by decapitation. The cerebral cortex was carefully separated from the entire brain for histopathological study. The isolated area was cleaned and cut into 0.5 cubic cm slices. After further fixation in 4%, paraformaldehyde in PBS PH= 7.4 overnight for (8–12 h) at room temperature, immersion in 70% ethanol was done. The tissue was stored at 37 °C until it was embedded in paraffin. The paraffin blocks were sliced into 4–5 m thickness using a rotary microtome. Hematoxylin and eosin were used to stain the sections, and morphology was examined using a fluorescent microscope (Type 102 M; ×100 Magnification). A fluorescence microscope was used to count the density of the normal neuronal population (Oligodendrocytes, astrocytes, and microglial cells) in the cerebral cortex in a blinded fashion using a reticular consolidated eyepiece at a magnification of ×100.

3. Statistical analysis

To assess the differences between treatment groups, data were analysed using two-way analysis of variance (ANOVA) followed by post-hoc Bonferroni's test, and one-way ANOVA repeated measures followed by post-hoc Tukey's multi comparison test. The body weight and other behavioural parameters were analysed using two-way ANOVA. In contrast, one-way ANOVA was used to analyze the relative brain-body weight ratio, demyelination volume, biochemical parameters, and TSTQ analysis. $P < 0.001$ was considered statistically significant. The data was confirmed to be normal, and the sample size was calculated using the Kolmogorov Smirnov test to check the normality distribution. The statistical analysis was done using GraphPad Prism software version 5.03 for Windows (GraphPad Software, San Diego, CA, USA). All the statistical results are presented as the mean and standard error of mean (SEM).

4. Results

4.1. Effect of α-mangostin in the restoration of weight variations in methylmercury-induced neurotoxicity in experimental rats

4.1.1. Improvement in body weight after chronic treatment with α-mangostin

Bodyweight was measured on the protocol schedule's 1st, 7th, 14th, 21st, 28th, 35th, and 42nd days. There was no statistically significant difference between any of the treatment groups on the first day. Compared to the normal control, vehicle control, and AMG200 mg/kg perse group, MeHg+ treated rats lost weight gradually on the 14th, 21st, 28th, 35th, and 42nd days. Compared to MeHg+ -treated rats on the 35th and 42nd days, continued treatment with AMG100 and 200 mg/kg resulted in a significant and dose-dependent increase in body weight [two-way ANOVA: $F(30,180) = 43.24$, $p < 0.001$]. Compared to the AMG100 mg/kg treatment group, AMG200 mg/kg showed a significant improvement in body weight restoration on days 35 and 42. (Fig. 2).

4.1.2. Improvement in ratios of brain/body weight after chronic treatment with α-mangostin

The relative brain-body weight ratio was measured on the 42nd day of the experiment to investigate the effect of AMG in MeHg+ -treated rats. Compared to the AMG perse group, there was no significant difference in the relative brain-body weight ratio between the normal and vehicle control groups. The relative brain-body weight ratio was significantly lower in the MeHg+ -treated group. Long-term oral AMG therapy at 100 mg/kg and 200 mg/kg doses enhanced the relative brain-body weight ratio considerably as compared to the MeHg+ -treated ALS group [one-way ANOVA: $F(5,25) = 0.257$, $p < 0.001$]. AMG200 mg/kg was also more effective than AMG100 mg/kg in restoring rats' relative brain-body weight ratio. (Fig. 3).

4.2. Neuroprotective effect of α-mangostin on behavioural changes in methylmercury-induced neurotoxicity in experimental rats

4.2.1. Improvement in memory and cognition after chronic treatment with α-mangostin

Escape latency time (ELT) was measured on the 39th, 40th, and 41st days of the experiment protocol schedule. MeHg+ treated rats showed a progressive increase in ELT compared to normal control, vehicle control,

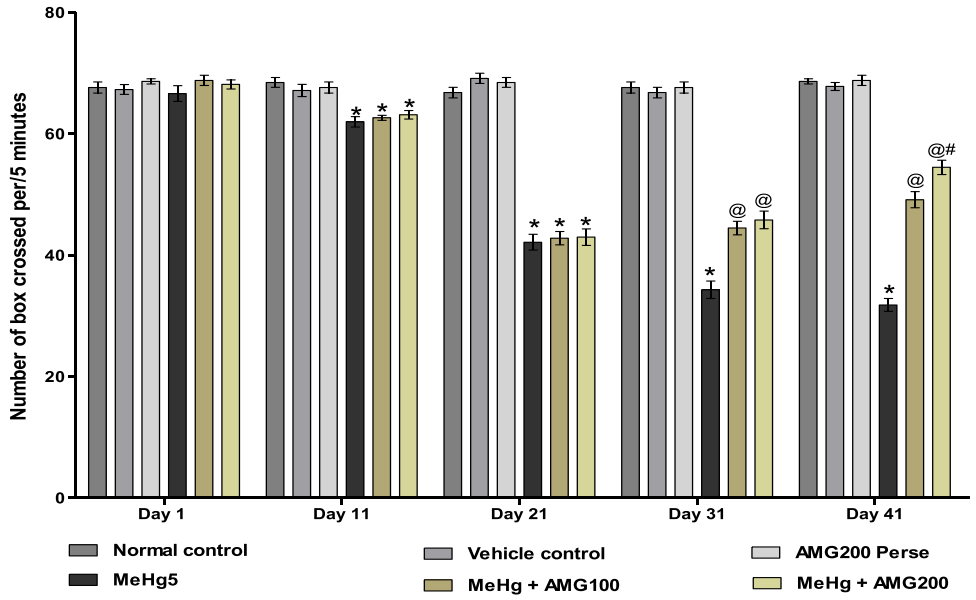

Fig. 6. Neuroprotective effect of α-mangostin on locomotion (number of boxes crossed) using open field test in methylmercury-induced neurotoxicity in experimental rats. Statistical analysis followed by two-way ANOVA (post-hoc Bonferroni's test), * $p < 0.001$ v/s normal control; vehicle control and AMG200 perse; @ $p < 0.001$ v/s MeHg5; @ # $p < 0.001$ v/s MeHg5 +AMG100; (n = 6 rats per group).

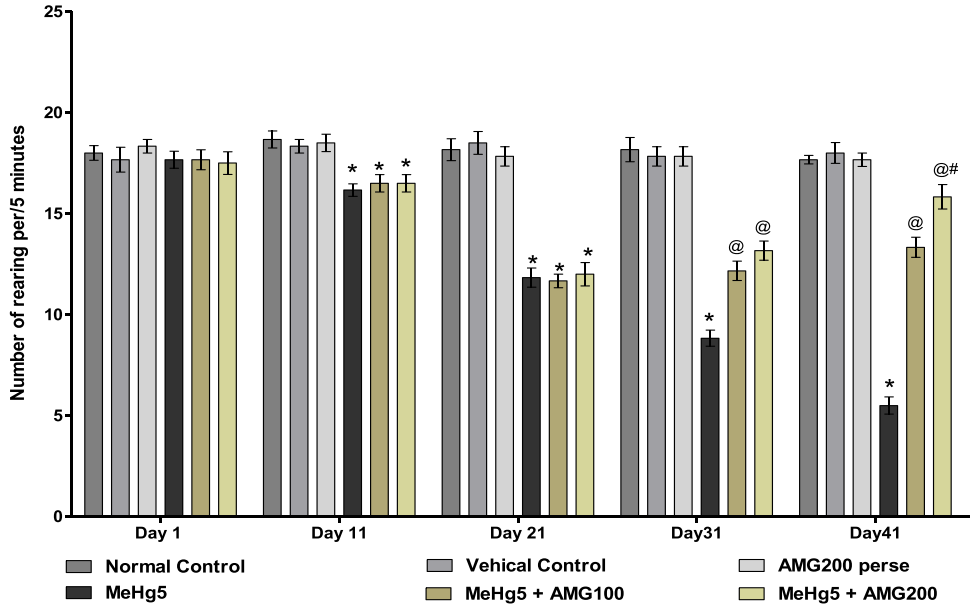

Fig. 7. Neuroprotective of effect α-mangostin on locomotion (number of rearing per/5 min) using open field test in methylmercury-induced neurotoxicity in experimental rats. Statistical analysis followed by two-way ANOVA (post-hoc Bonferroni's test), * $p < 0.001$ v/s normal control; vehicle control and AMG200 perse; @ $p < 0.001$ v/s MeHg5; @ # $p < 0.001$ v/s MeHg5 +AMG100; (n = 6 rats per group).

and AMG200 perse treated rats. When compared to the MeHg+ treated group, prolonged AMG100 mg/kg and AMG200 mg/kg treatment significantly reduces ELT [two-way ANOVA: $F(10,60) = 15.26$, $p < 0.001$]. Compared to the AMG100 mg/kg treated group, AMG200 mg/kg exhibited an effective decrease in ELT. (Fig. 4).

The time spent in the target quadrant (TSTQ) was measured on day 42. TSTQ decreased gradually in MeHg+ -induced ALS animals compared to normal controls, vehicle controls, and AMG200 perse. When compared to the MeHg+ -treated group, prolonged AMG100 and 200 mg/kg administration significantly raised TSTQ in the Morris water maze task [one-way ANOVA: $F(5,25) = 0.369$, $p < 0.001$]. Compared to the AMG100 mg/kg treatment group, AMG200 mg/kg was more effective and significantly improved TSTQ on day 42. (Fig. 5).

4.2.2. Increased locomotion and reduced anxiety after chronic treatment with α-mangostin

Locomotor and rearing behaviour were observed on the treatment regimen's 1st, 11th, 21st, 31st, 34th and 41st days. The number of boxes crossed and reared by MeHg+ -induced ALS rats was measured in an open field test. Rats given MeHg+ showed a progressive decrease in locomotor activity and an increase in rearing activity compared to normal vehicle control and AMG200 mg/kg perse treated rats. Prolonged oral administration of AMG100 and 200 mg/kg significantly enhanced locomotor activity [two-way ANOVA: $F(20,120) = 58.55$, p0.001] and decreased anxiety [two-way ANOVA: $F(20,120) = 23.80$, p0.001] as compared to the normal, vehicle control, and AMG200 treatment groups. Compared to AMG100 mg/kg treated rats,

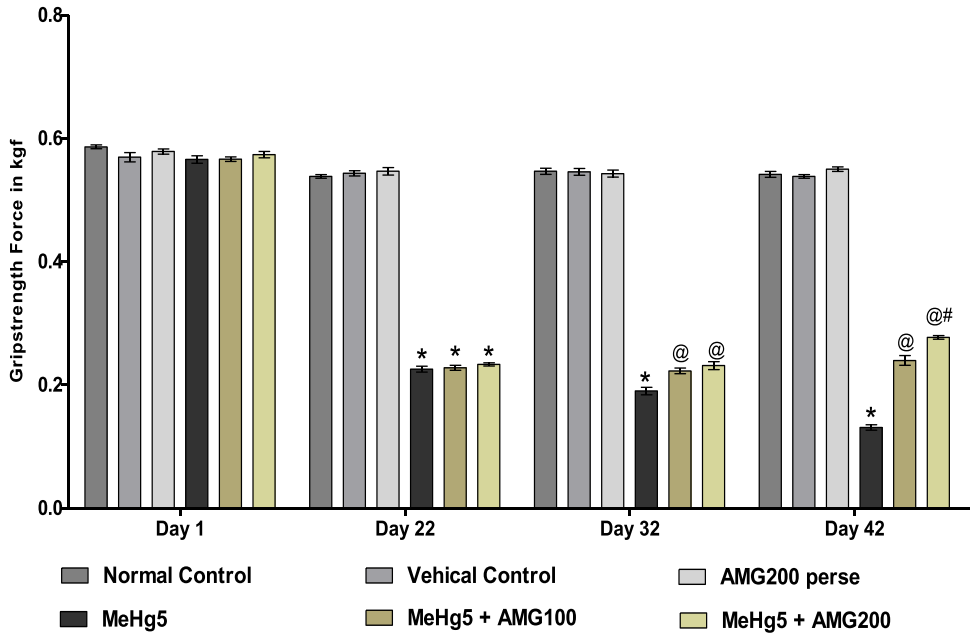

Fig. 8. Neuroprotective effect of α-mangostin on grip strength test in methylmercury-induced neurotoxicity in experimental rats. *S*tatistical analysis followed by two-way ANOVA (post-hoc Bonferroni's test), * $p < 0.001$ v/s normal control; vehicle control and AMG200 perse; @ $p < 0.001$ v/s MeHg5; @ # $p < 0.001$ v/s MeHg5 +AMG100; (n = 6 rats per group).

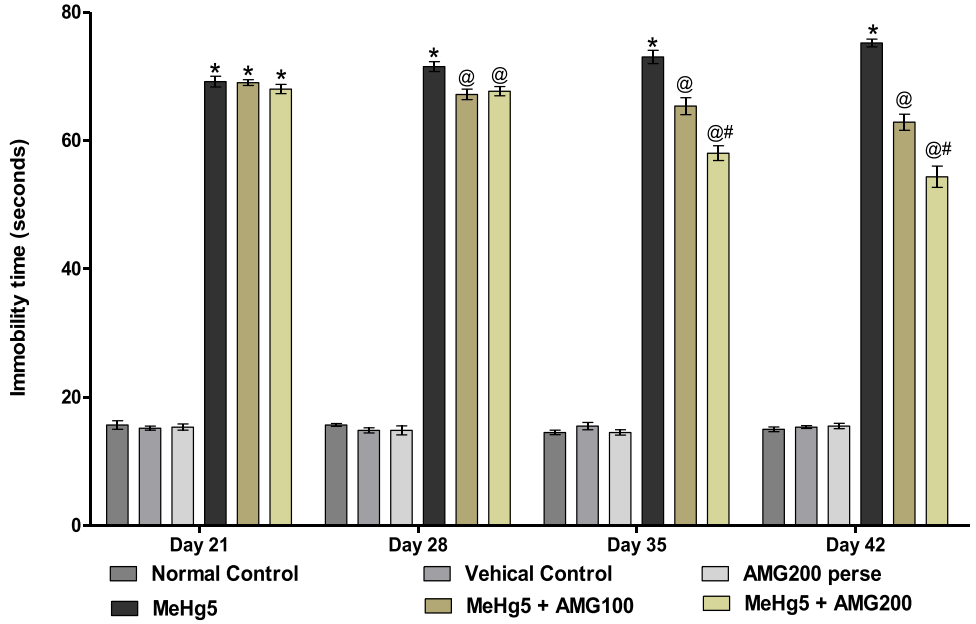

Fig. 9. Neuroprotective effect of α-mangostin on forced swim test (Immobility time) using in methylmercury-induced neurotoxicity in experimental rats. Statistical analysis followed by two-way ANOVA (post-hoc Bonferroni's test), * $p < 0.001$ v/s normal control; vehicle control and AMG200 perse; @ $p < 0.001$ v/s MeHg5; @ # $p < 0.001$ v/s MeHg5 +AMG100; (n = 6 rats per group).

AMG200 mg/kg was more efficacious and significantly improved locomotion and rearing activities on day 41. (Figs. 6, 7).

4.2.3. Improved grip strength after chronic treatment with α-mangostin

The grip strength activity was completed on the protocol's 1st, 22nd, 32nd, and 42nd days. No significant difference was discovered between normal control, vehicle control, and AMG perse group on the first day. MeHg+ -treated rats had considerably lower grip strength force on the 22nd day than the normal control, vehicle control, and AMG200 perse group. Compared to MeHg+ -treated ALS rats, animals treated with AMG100 mg/kg and 200 mg/kg on the 32nd and 42nd day improved grip strength force considerably and dose-dependently [two-way ANOVA: $F(15,90) = 337.7$, p0.001]. Compared to AMG100 mg/kg treated rats, AMG200 mg/kg was more effective and significantly enhanced grip strength on day 42. (Fig. 8).

4.2.4. Reduced depression-like behaviour after chronic treatment with α-mangostin

Immobility time was measured using a forced swim test on the 21st, 28th, 35th, and 42nd days of the experimental schedule. The MeHg+ -treated ALS rats exhibited depressive-like behaviour compared to the normal control, vehicle control, and AMG200 perse treated ra and

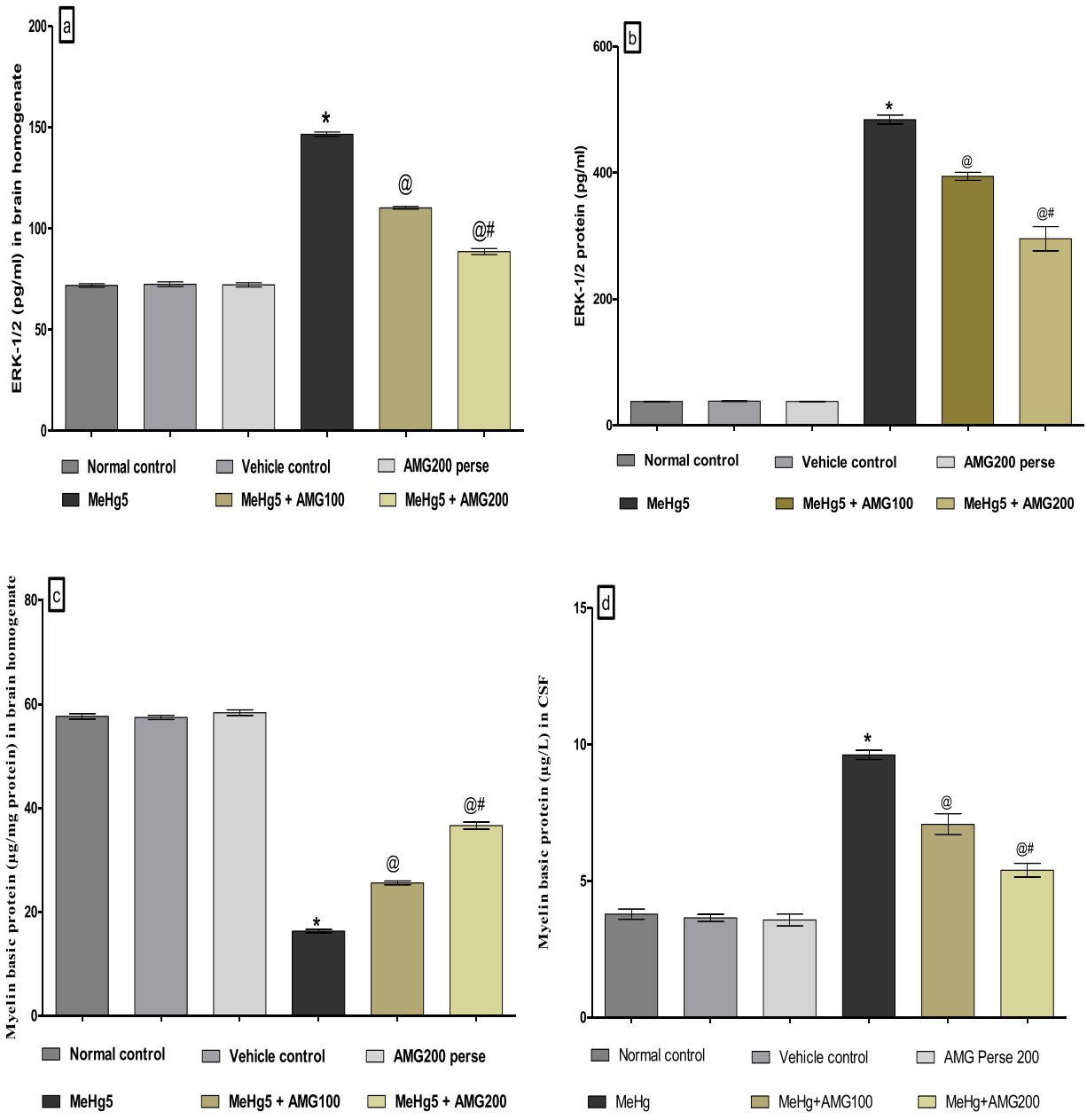

Fig. 10. Neuroprotective effect of α-mangostin on ERK-1/2 and myelin basic protein level in methylmercury-induced neurotoxicity in experimental rats (a-d). Statistical analysis followed by one-way ANOVA (post-hoc Tukey's test), * $p < 0.001$ v/s normal control; vehicle control and AMG200 Perse; @ $p < 0.001$ v/s MeHg5; @ # $p < 0.001$ v/s MeHg5 + AMG100; (n = 6 rats per group).

gradually increased immobility time. Long-term administration of AMG100 mg/kg and 200 mg/kg significantly reduced immobility time on days 28th, 35th, and 42nd when compared to the normal control, vehicle control, and AMG200 perse treatment groups [two-way ANOVA: $F(15,90) = 19.12$, $p < 0.001$]. AMG200 mg/kg significantly reduced immobility score on the 35th and 42nd days compared to AMG100mg/kg treatment group. (Fig. 9).

4.3. Neuroprotective effect of α-mangostin on neurochemical changes in methylmercury-induced neurotoxicity in experimental rats

4.3.1. Decrease ERK-1/2 level after chronic treatment with α-mangostin

The level of ERK-1/2 protein in rat brain homogenates and CSF was measured at the end of the experiment. ERK-1/2 protein levels were significantly higher in MeHg+ -treated rats compared to normal, vehicle control, and AMG200 perse-treated rats. The levels of ERK-1/2 protein in brain homogenate were considerably and dose-dependently decreased by oral administration of AMG100 mg/kg and 200 mg/kg [one-way ANOVA: $F(5,25) = 0.157$, $p < 0.001$] and CSF samples [one-way ANOVA: $F(5,25) = 0.675$, $p < 0.001$] compared to MeHg+ treated group. AMG200 mg/kg was more efficient than AMG100 mg/kg in reducing ERK-1/2 protein in brain homogenate and CSF. (Fig. 10).

4.3.2. Restoration in myelin basic protein level after chronic treatment with α-mangostin

An ELISA kit measured Myelin basic protein (MBP) in rat brain homogenate and CSF. Compared to the control, vehicle, and AMG200 mg/kg perse treated groups, long-term oral administration of MeHg+ to rats substantially reduced MBP levels in brain homogenate and increased CSF samples. Continued oral administration of AMG at doses of 100 mg/kg and 200 mg/kg substantially elevated the amount of MBP protein in brain homogenate [one-way ANOVA: $F(5,25) = 1.040$, $p < 0.001$] and

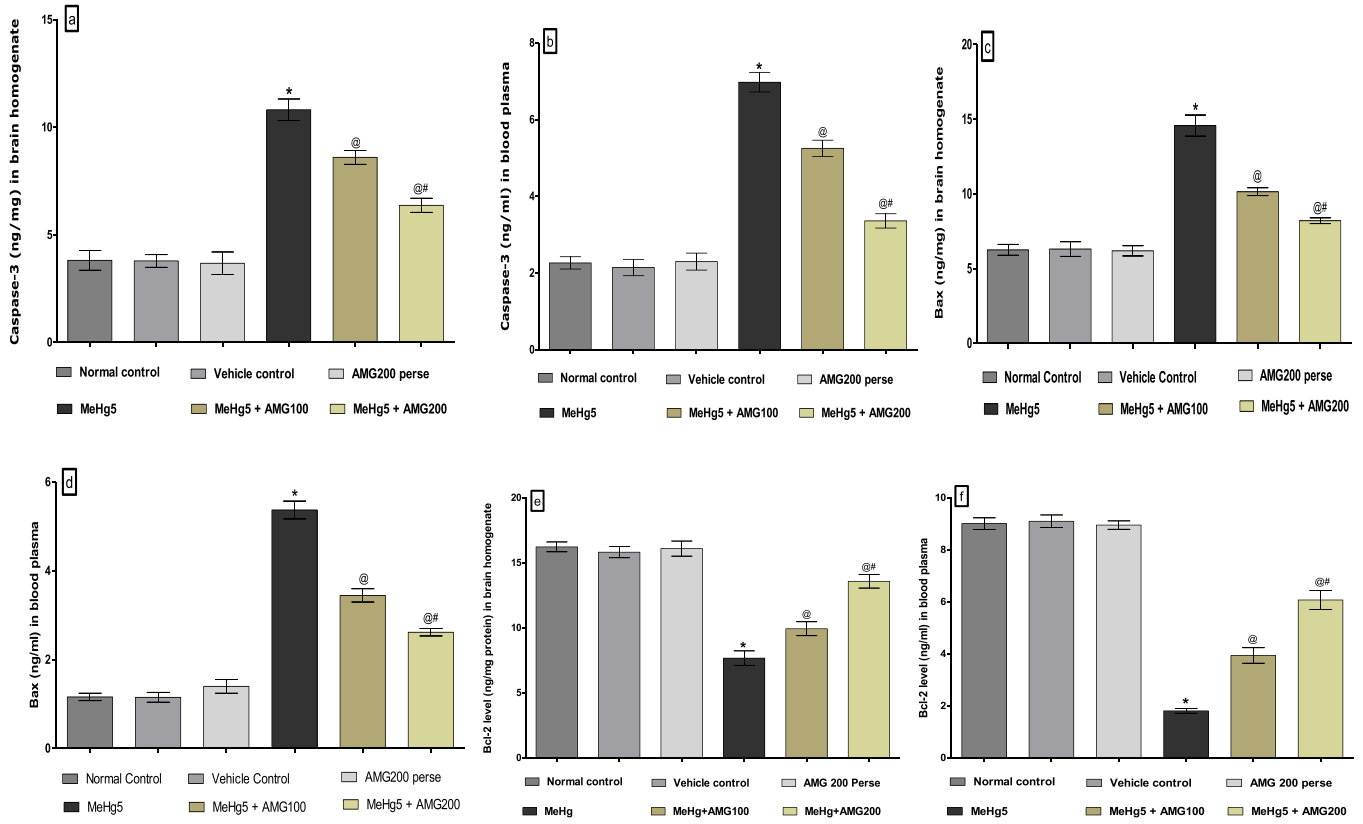

Fig. 11. Neuroprotective effect of α-mangostin on caspase-3, Bax, and Bcl-2 levels in methylmercury-induced neurotoxicity in experimental rats (a-f). Statistical analysis followed by one-way ANOVA (post-hoc Tukey's test), * $p < 0.001$ v/s normal control; vehicle control and AMG200 Perse; @ $p < 0.001$ v/s MeHg5; @ # $p < 0.001$ v/s MeHg5 + AMG100; (n = 6 rats per group).

decreased in CSF samples [one-way ANOVA: $F(5,25) = 0.778$, $p < 0.001$] compared to MeHg+ treated rats. Compared to the AMG100 mg/kg treatment group, AMG200 mg/kg significantly increased MBP restoration in brain homogenate and CSF. (Figs. 10a to d).

4.3.3. Decreased caspase-3, Bax, and increased Bcl-2 levels after chronic treatment with α-mangostin

At the end of the study, the levels of apoptotic markers Caspase-3, Bax, and Bcl-2 in rat brain homogenate and blood plasma. Compared to normal, vehicle control, and AMG200 mg/kg perse-treated rats, MeHg+ -treated rats had significantly higher caspase-3, Bax, and lower Bcl-2 levels in brain homogenate and blood plasma. In brain homogenate, oral administration of AMG at dosages of 100 mg/kg and 200 mg/kg significantly decreased caspase-3 [one-way ANOVA: $F(5,25) = 0.392$, $p < 0.001$], Bax [one-way ANOVA: $F(5,25) = 1.174$, $p < 0.001$], and increased Bcl-2 [one-way ANOVA: $F(5,25) = 0.825$, $p < 0.001$].

After the study, the apoptotic markers Caspase-3, Bax, and Bcl-2 in rat brain homogenate and blood plasma were measured. MeHg+ -treated rats had significantly higher caspase-3, Bax, and lower Bcl-2 levels in brain homogenate and blood plasma when compared to normal, vehicle control, and AMG200 mg/kg perse-treated rats. Oral treatment of AMG at 100 mg/kg and 200 mg/kg significantly lowered caspase-3 [one-way ANOVA: $F(5,25) = 0.392$, $p < 0.001$], Bax [one-way ANOVA: $F(5,25) = 1.174$, $p < 0.001$], and raised Bcl-2 [one-way ANOVA: $F(5,25) = 0.825$, $p < 0.001$] in brain homogenate. (Figs. 11a to f).

4.3.4. Restoration of neurotransmitter level after chronic treatment with α-mangostin

Neurotransmitter levels in rat brain homogenate were measured at the end of the experiment, including GABA, serotonin, acetylcholine, and glutamate. MeHg+ -ALS rats observed a significant decrease in GABA, acetylcholine serotonin, and an enhanced glutamate level in the brain homogenate compared to normal control, vehicle control, and AMG200 perse treated rats.Chronic oral treatment of AMG100 mg/kg and 200 mg/kg substantially and dose-dependently increases GABA [one-way ANOVA: $F(5,25) = 0.888$, $p < 0.001$], acetylcholine [one-way ANOVA: $F(5,25) = 0.895$, $p < 0.001$], serotonin [one-way ANOVA: $F(5,25) = 2.691$, $p < 0.001$], and decreases glutamate [one-way ANOVA: $F(5,25) = 1.617$, $p < 0.001$] When compared to the AMG100 mg/kg treated group, the AMG200 mg/kg group significantly restored neurotransmitter levels (Figs. 12a to d).

4.3.5. Restored neuroinflammatory levels after chronic treatment with α-mangostin

To explore the therapeutic effect of AMG in MeHg+ -treated rats, we measured the levels of neuroinflammatory biomarkers such as TNF-α and IL-1β in rat brain homogenate, and blood plasma. TNFα - and IL-1β levels in blood plasma and brain homogenate were considerably greater in MeHg+ -treated rats than in normal controls, vehicle controls, and AMG200 mg/kg perse group. Long-term oral treatment with AMG100 mg/kg and 200 mg/kg for 21 days reduced TNF-α [one-way ANOVA: $F(5,25) = 1.119$, $p < 0.001$] and IL-1β levels [one-way ANOVA: $F(5,25) = 1.369$, $p < 0.001$] in brain homogenate, as well as decreased TNF-α [one-way ANOVA: $F(5,25) = 0.248$, $p < 0.001$] and IL-1β [one-way ANOVA: $F(5,25) = 0.450$, $p < 0.001$] level in blood plasma.

TNF- and IL-1 levels were considerably lower in the AMG200 mg/kg group compared to the AMG100 mg/kg group in whole-brain homogenate and blood plasma. TNF- and IL-1 levels in whole brain homogenate and blood plasma were significantly lower in the AMG200 mg/kg group than in the AMG100 mg/kg group (Figs. 13a to d).

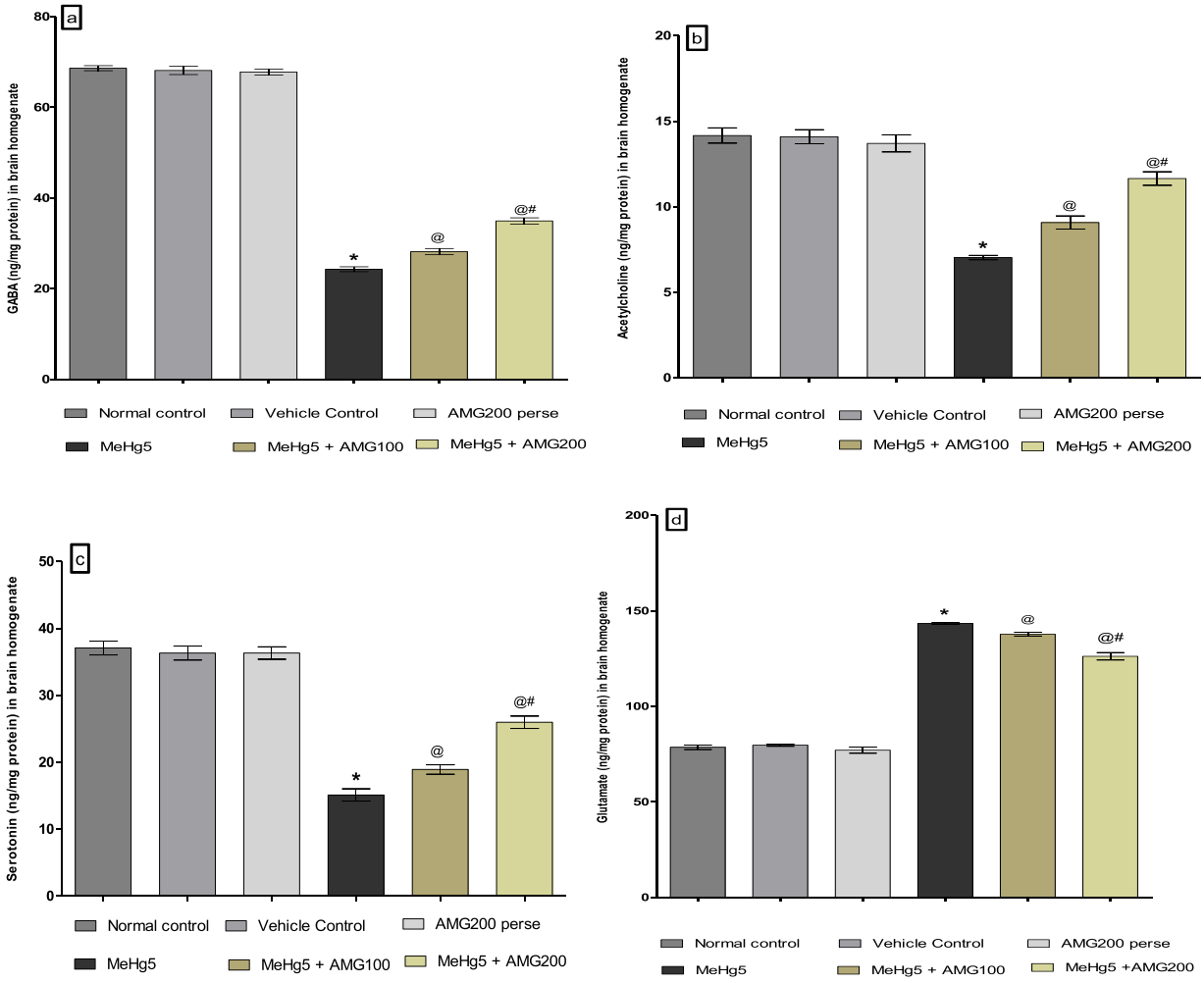

Fig. 12. Neuroprotective effect of α-mangostin on neurotransmitters level in methylmercury-induced neurotoxicity in experimental rats (a-d). Statistical analysis followed by one-way ANOVA (post-hoc Tukey's test), * $p < 0.001$ v/s normal control; vehicle control and AMG200 Perse; @ $p < 0.001$ v/s MeHg5; @ # $p < 0.001$ v/s MeHg5 + AMG100; (n = 6 rats per group).

4.3.6. *Restored antioxidants levels after chronic treatment with α-mangostin*

The oxidative stress indicators AchE, MDA, LDH, GSH, SOD, and nitrite, were measured in whole rat brain homogenate. In comparison to the normal control, vehicle control, and AMG200 perse group, oral treatment of MeHg+ rats resulted in significantly lower SOD and GSH levels, as well as elevated AchE, MDA, LDH, and nitrite levels in brain homogenate. The oral administration of AMG100 mg/kg and 200 mg/kg decreased level of AchE [one-way ANOVA: $F(5,25) = 1.175$, $p < 0.001$], MDA [one-way ANOVA: $F(5,25) = 1.280$, $p < 0.001$], LDH [one-way ANOVA: $F(5,25) = 0.567$, $p < 0.001$], and nitrite [one-way ANOVA: $F(5,25) = 6.166$, $p < 0.001$] and increased the level of SOD [one-way ANOVA: $F(5,25) = 0.873$ $p < 0.001$]and GSH [one-way ANOVA: $F(5,25) = 1.726$, $p < 0.001$] in $MeHg^{+}$ treated rats. AMG200 mg/kg significantly restored antioxidant levels in brain homogenate compared to AMG100 mg/kg treatment group. (Figs. 14a to f).

4.4. *Neuroprotective effect of α-mangostin on gross pathological evaluation in methylmercury-induced neurotoxicity in experimental rats*

4.4.1. *Improvement in whole-brain pathological alterations after chronic treatment with α-mangostin*

MeHg+ -treated brain rats displayed morphological abnormalities such as changes in size and form, decreased overall brain mass, degeneration of sulci, motor neurons, and meninges breaking compared to the normal control, vehicle control, and AMG200 perse group. Long-term oral AMG treatment at doses of 100 mg/kg and 200 mg/kg repaired the morphological defects in MeHg+ -treated rats. AMG200 mg/kg had a more significant effect than AMG100 mg/kg in treating gross pathological abnormalities in MeHg+ -treated rats. (Fig. 15).

4.4.2. *Reduction of pathological changes in brain sections after chronic treatment with α-mangostin*

All rats were sacrificed following the behavioural testing, and fresh brain sections were separated for morphological examination. Oral MeHg+ treatment of rat brain sections revealed a damaged, demyelinated zone associated with white matter tissue degeneration, resulting in severe damage in the cerebral cortex, basal ganglia, and hippocampus tissue compared to normal control vehicle control and AMG200 perse treated groups. In MeHg+ -treated rats, chronic AMG100 mg/kg and 200 mg/kg therapy effectively repaired demyelinated regions and reduced pathological alterations. In MeHg+ -treated rats, AMG200 mg/kg was more efficient than AMG100 mg/kg in decreasing pathological changes. (Fig. 16).

4.4.3. *Reduced demyelination volume after long term administration with α-mangostin*

The normal control, vehicle control, and AMG200 perse groups had no statistically significant influence on the size of the demyelination area when compared to MeHg+ -treated rats. Long-term oral MeHg+

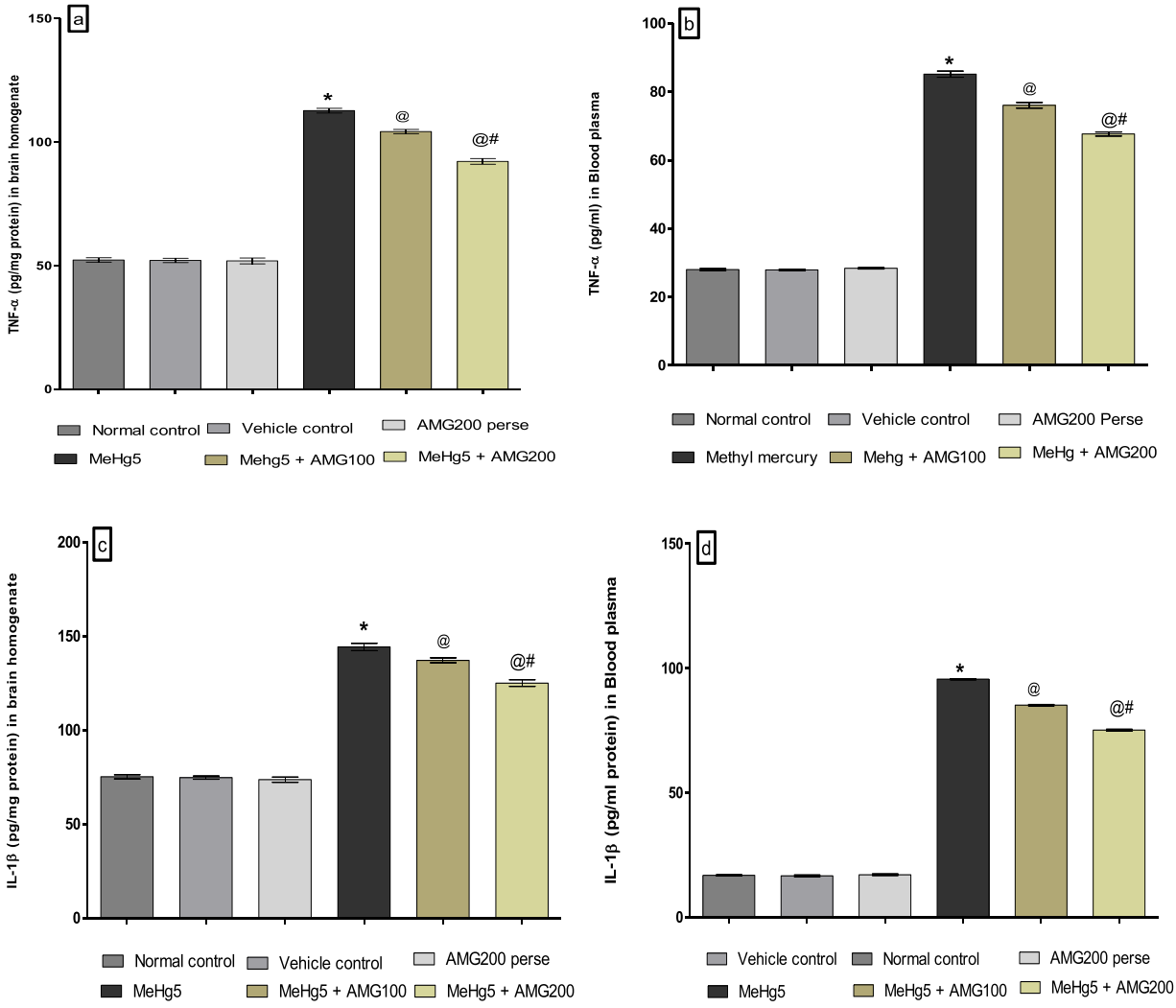

Fig. 13. Neuroprotective effect of α-mangostin on amelioration of inflammatory level in methylmercury-induced neurotoxicity in experimental rats (a-d). Statistical analysis followed by one-way ANOVA (post-hoc Tukey's test), * $p < 0.001$ v/s normal control; vehicle control and AMG200 Perse; @ $p < 0.001$ v/s MeHg5; @ # $p < 0.001$ v/s MeHg5 + AMG100; (n = 6 rats per group).

therapy resulted in a significant increase in demyelination volume in rats.Chronic AMG100 mg/kg and 200 mg/kg administration significantly reduced demyelination volume [one-way ANOVA: $F(5,25) = 0.270$, $p < 0.001$] when compared to normal, vehicle control, and AMG200 mg/kg perse group. Compared to AMG100 mg/kg treated rats, AMG200 mg/kg demonstrated a significant and dose-dependent restoration and reduction in demyelination volume (Fig. 17).

4.5. Neuroprotective effect of α-mangostin in methylmercury-induced histopathological changes

The vehicle control, sham control, and AMG perse treated groups all had normal morphology of cerebral cortical neurons, as indicated by rod-shaped microglial cells, healthy oligodendrocytes, and normal astrocytes. The MeHg+ group showed oligodendrocyte cell death, microglial activation, and increased astrocyte density. AMG observed a progressive restoration in the oligodendrocyte cells and a significant decrease in the number of astrocytes at a dose of 100 mg/kg. AMG 200 mg/kg restored oligodendrocyte cell shape while lowering microglia and astrocyte activation (Fig. 18).

5. Discussion

The current study looks into AMG's neuroprotective potential in MeHg+ -induced rats. $MeHg^{+}$ is a well-known environmental neurotoxin that causes oxidative damage and indirect excitotoxicity due to altered glutamate metabolism [94]. MeHg+ is an environmental neurotoxin; exposure may raise the incidence of neurotoxicities such as neurodegenerative diseases and cognitive impairment [95]. The MeHg+-cysteine amino acid combination, like methionine amino acid, allows oral MeHg+ treatment to enter the CNS. Because MeHg+ is lipophilic, it quickly diffuses from the blood into the CNS as a cysteine complex across the blood-brain barrier (BBB) via the L-type neutral amino acid carrier transport (LAT) system [96]. $MeHg^{+}$ caused a wide range of neurons to become hypoplastic, aberrant, and disoriented, indicating that migration, maturation, and growth were disrupted, and the resulting $MeHg^{+}$-treated rat model. It is associated with motor function impairment, loss of muscle control, and memory impairment in the rat [97].

According to clinical, experimental, and epidemiological research, mercury may play a critical role in the etiology of ALS [10], as well as other neurological disorders such as multiple sclerosis [98] and Alzheimer's disease [99]. $MeHg^{+}$ exposure causes NMDA receptor overactivation, which increases Ca2+ influx into neuronal cells and activates

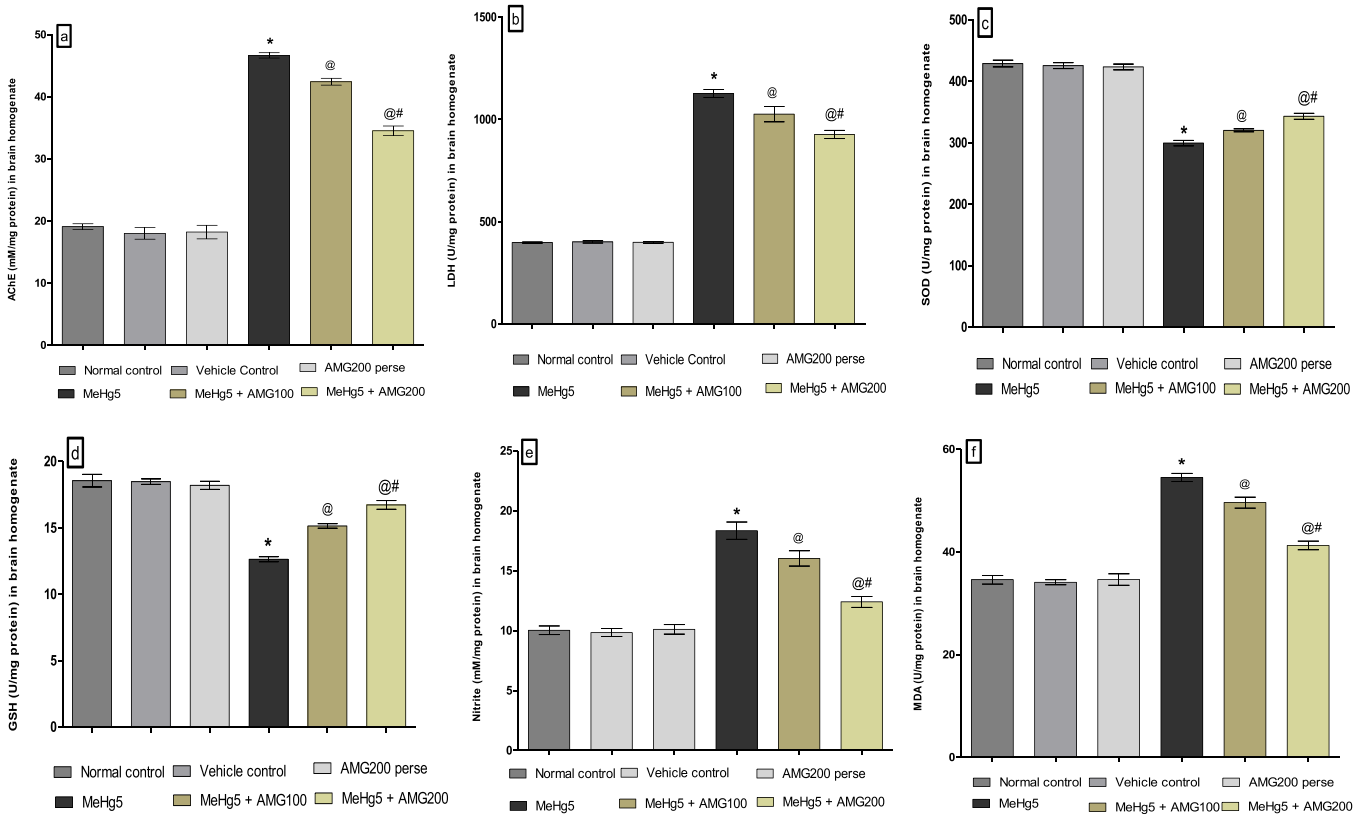

Fig. 14. Neuroprotective effect of α-mangostin on ameliorating oxidative stress markers level in methylmercury-induced neurotoxicity in experimental rats (a-f). Statistical analysis followed by one-way ANOVA (post-hoc Tukey's test), * $p < 0.001$ v/s normal control; vehicle control and AMG200 Perse; @ $p < 0.001$ v/s MeHg5; @ # $p < 0.001$ v/s MeHg5 + AMG100; (n = 6 rats per group).

apoptosis pathways. Ca2+ also influxes in mitochondria, inducing reactive oxygen species (ROS) [100].

Mutations in SOD-1 protein expression elicited ALS-like symptoms in a MeHg+ -induced animal model, such as early signs of hind limb paralysis in mice [101]. This study aims to investigate the neuroprotective potential of AMG in MeHg+ -treated rats. Various neurobehavioral tests, including cellular and molecular markers, neurotransmitters, apoptotic markers, neuroinflammatory cytokine levels, and oxidative stress parameters, were investigated in rat brain homogenate, blood plasma, and CSF samples.

Prolonged oral treatment of AMG at doses of 100 mg/kg and 200 mg/kg elicited a neuroprotective effect against motor neuron abnormalities and neurological abnormalities in rats treated with MeHg+. According to our findings, MeHg+ -treated rats significantly lost body weight and had a lower relative brain-body weight ratio. Furthermore, unlike MeHg+ -induced animals, the rats' bodyweight was significantly restored with continued oral AMG therapy.

The open-field test evaluates locomotor and anxiety-like behaviour and confirms the neurological basis of pharmacological target and anxiolytic drug screening [102,103]. We used the open-field test to examine motor activity and exploratory behaviour changes in rats. The MeHg+ exposure reduced the number of boxes crossed and rearings. Furthermore, in MeHg+ -treated rats, oral AMG treatment significantly reduced motor impairment and anxiety-like symptoms.

The grip strength experiment was carried out to look at differences in neuromuscular abilities in rats [104]. Grip strength is being used as a diagnostic tool in the medical field to diagnose motor dysfunctions. According to research, there is a link between grip strength and the strength of other muscular motions in healthy and unwell people, and it is the most effective tool [105,106]. MeHg+ treatment rats had considerably reduced muscular function, as seen by decreased locomotor activity and a significant loss in grip strength. According to our findings, grip strength was significantly reduced in MeHg+ -treated rats. In MeHg+ -treated rats, the AMG-treated group significantly improved the loss of forelimb and hindlimb grip strength.

FST is a widely used test in scientific and preclinical research to assess the efficacy of antidepressant medications as well as the impact of various behavioural and neurobiological changes in rats and mice [107,108]. MeHg+ -treated rats in FST exhibited immobility and depressive-like behaviour in previous studies [109]. According to our findings, long-term AMG therapy reduces immobility and depressive-like behaviour in MeHg+ -treated rats, showing that AMG has neuroprotective effects on brain function restoration.

The MWM is a well-known and commonly used behavioural test for testing memory and cognitive skills[110]. MWM performance has also been connected to long-term potentiation and NMDA receptor activation, making it effective for examining hippocampal function [111]. Previous research has demonstrated that $MeHg^{+}$negatively influences synaptic activity, cognition, and memory in preadolescent rats [112]. This study aims to investigate the effect of AMG on memory and cognitive impairment in MWM. Oral $MeHg^{+}$ administration significantly increased ELT and decreased TSTQ in $MeHg^{+}$-treated rats, resulting in severe neuromuscular deficits and cognitive impairments [6]. In the current study, continuous AMG therapy restored memory, cognitive impairment, and neurological dysfunction in $MeHg^{+}$-treated rats.

The ERK-1/2 signalling pathway involves essential biological functions, including cell proliferation, survival, differentiation, motility, and cell death [39]. Previous research has associated ERK-1/2 signalling pathway alterations to ALS development and related neurocomplications [38,113]. ALS is characterised by glial cell overactivation, oligodendrocyte death, glutamate excitotoxicity, neuroinflammation, and neurotransmitter dysfunction caused by abnormal ERK-1/2 signalling [114,115]. The effect of AMG on ERK-1/2 signalling was studied to

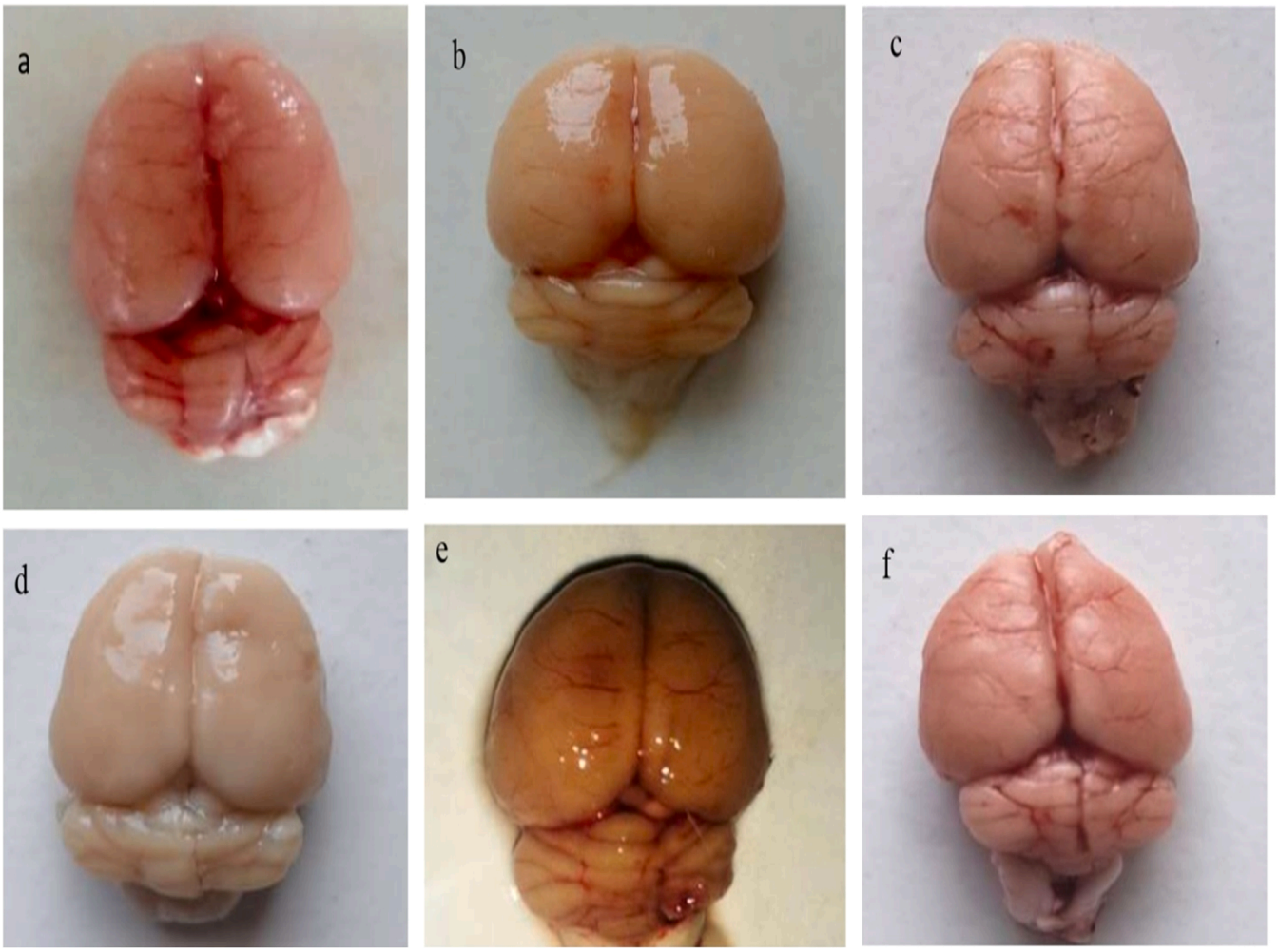

Fig. 15. Neuroprotective effect of α-mangostin on gross pathological changes (Whole brain) in methylmercury-induced neurotoxicity in experimental rats. Normal control (b) Vehicle control (c) AMG200 perse (d) $MeHg^{+}5$ (e) $MeHg^{+}5$ + AMG100 (f) $MeHg^{+}5$ + AMG200.

uncover the cellular and molecular pathways that support AMG's role in neuroprotection. ERK-1/2 levels in rat brain homogenate and CSF were measured using an ELISA kit. The oral AMG treatment reduced ERK-1/2 levels considerably. These findings suggest that AMG can regulate ERK/1/2 signalling dysregulation in damaged neuronal cells.

Oligodendrocytes are neuroglia whose major role in the central nervous system nourishes and insulates axons [116]. Myelination is primarily defined as the recurrent growth of axons by MBP-produced oligodendrocytes. MBP interacts with lipids in the myelin membrane to help keep the structure of the myelin stable [117]. A significant pathogenic component of ALS pathogenesis is myelin sheath degeneration, mediated by a continuous decline in MBP levels. Demyelination has been linked to motor dysfunction, neurological difficulties, diminished cognitive abilities, and poor nerve impulse conduction [118,119].

Neuronal cell death and neurodegenerative illnesses are caused by white matter demyelination, which is regarded to be a diagnostic sign of ALS. Furthermore, OPCs appear to be disrupted in ALS patients' brain and spinal cords, with demyelination regions indicating oligodendrocyte death and abnormal axon remyelination [120-122]. MBP, a myelin sheath protein, and monocarboxylate transporter-1 (MCT1) expression are significantly reduced, indicating a distinct loss of oligodendrocyte function [123,124].

The current research found that a 5 mg/kg oral dose of MeHg+ caused significant alterations in MBP concentrations in rat brain homogenate and CSF. In contrast, AMG's continuous therapy restored significantly altered MBP levels in the relevant biological samples. According to our findings, AMG may have an essential role in the remyelination of axonal neurons and preventing white matter damage caused by the MeHg+ neurotoxin in rats. These findings are critical for comprehending the relationship between AMG and neuropathogenic processes. More research into the molecular pathways that support such neuroprotective effects is essential.

Apoptosis, also known as programmed cell death, is necessary for the development of the peripheral and central nervous systems and proliferative tissues like the skin, intestinal mucosa, and immune system [125]. Many pathogenic mechanisms, including glutamate-mediated excitotoxicity and oxidative stress, can impair neuronal function, resulting in motor neuron cellular death [126,127].

In rat brain homogenate and blood plasma samples, a recent study observed that oral MeHg+ administration enhanced pro-apoptotic markers such as caspase-3 and Bax while decreasing anti-apoptotic markers such as Bcl-2. Our findings show that long-term AMG therapy reverses apoptotic markers in rat brain homogenate and blood plasma. These promising findings suggest that AMG may delay the progressive loss of motor neurons in ALS like a neurodegenerative disease. Neurotransmitters are generally referred to as the body's chemical messengers. They are the substances that the nervous system uses to interact with neurons and muscles [128]. A neurotransmitter impacts neurons in three ways: excitatory, inhibitory, or modulatory. An excitatory neurotransmitter induces the production of electrical impulses known as action potentials in the neurological system, whereas an inhibitory neurotransmitter suppresses it [129].

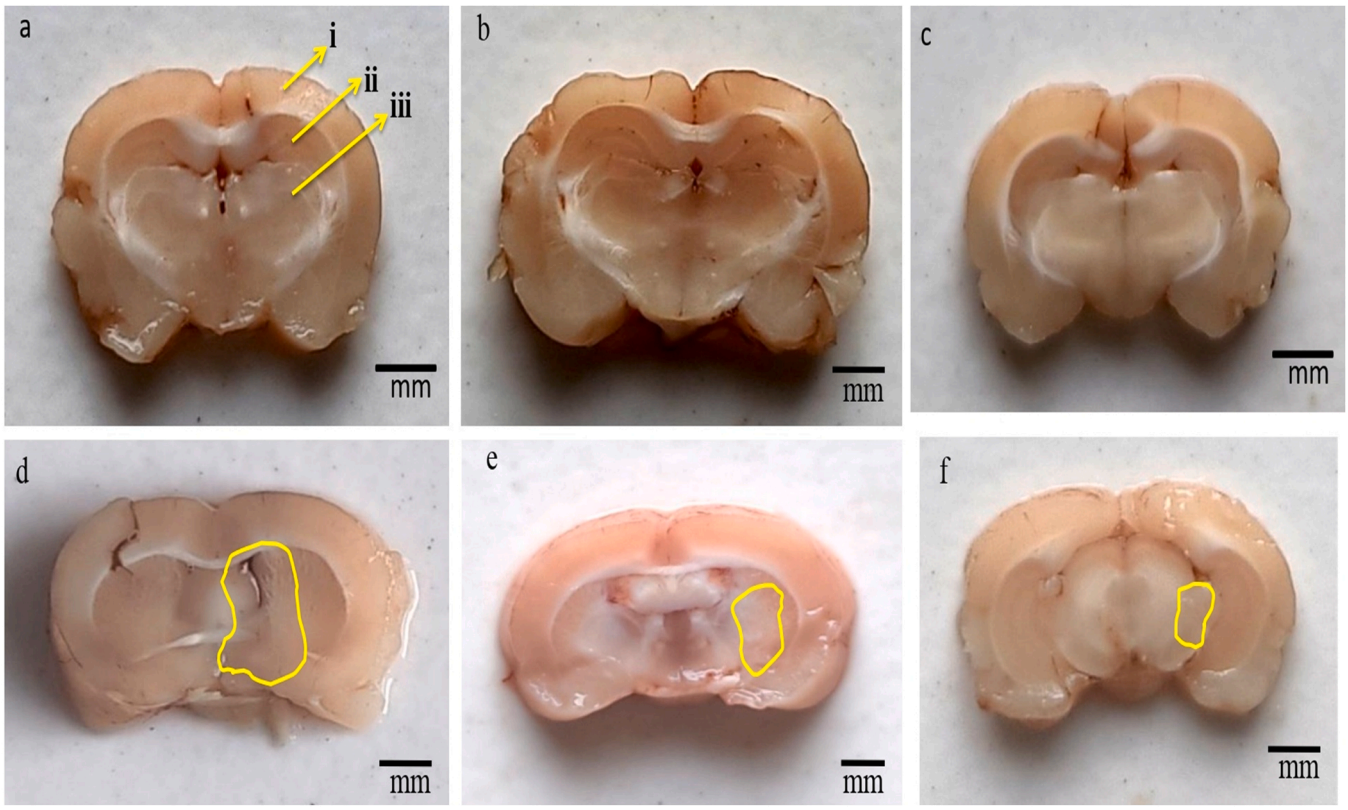

Fig. 16. Neuroprotective effect of alpha-mangostin on gross pathological changes (brain section) in methyl mercury-induced neurotoxicity in experimental rats. Normal control:- i) Cerebral cortex ii) Hippocampus iii) Basal ganglia (b) Vehicle control (c) AMG200 perse (d) $MeHg^{+}5$ (e) $MeHg^{+}5$ + AMG100 (f) $MeHg^{+}5$ + AMG200. **Note:** Yellow circles are pointing to the site of the brain injury (Scale bar = 2 mm).

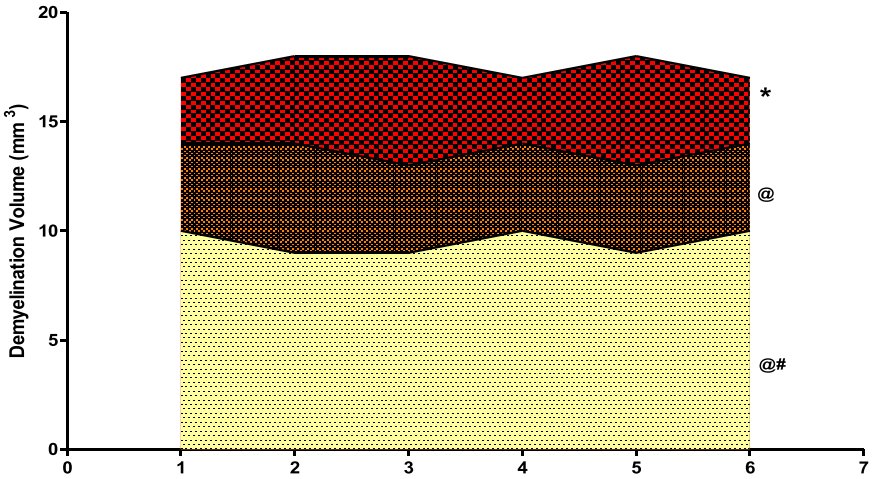

Fig. 17. Neuroprotective effect of α-mangostin on demyelination volume in methylmercury-induced neurotoxicity in experimental rats. Statistical analysis followed by one-way ANOVA (post-hoc Tukey's test), * $p < 0.001$ v/s normal control; vehicle control and AMG200 Perse; @ $p < 0.001$ v/s MeHg5; @ # $p < 0.001$ v/s MeHg5 + AMG100; (n = 6 rats per group).

Previous research suggests that excitatory and inhibitory neurotransmitter imbalances may contribute to ALS and other neurological abnormalities in rats [130,131]. Park and colleagues previously proposed that excitatory neurotransmitters such as glutamate are involved in oligodendrocyte or glial cell death and may contribute to white matter degeneration [132]. Long-term and dose-dependent therapy of AMG rats against MeHg+ -treated rats considerably restored neurotransmitter levels such as GABA, acetylcholine, serotonin, and glutamate in rat brain homogenate.

Microglial activation accelerates the inflammatory process by activating pro-inflammatory cytokines and signalling pathways, resulting in synaptic damage, neuronal death, and the activation of other proinflammatory cytokines [133]. These pro-inflammatory cytokines may play a variety of roles in neurodegeneration and neuroprotection, including the use of helpful pro-inflammatory cytokines and the regulation of damaging pro-inflammatory cytokines produced by microglia in neurodegenerative diseases [134].

TNF- and IL-1 levels were measured in the brain homogenate and blood plasma of MeHg+ -treated rats. Furthermore, long-term AMG administration at 100 mg/kg and 200 mg/kg dosages significantly

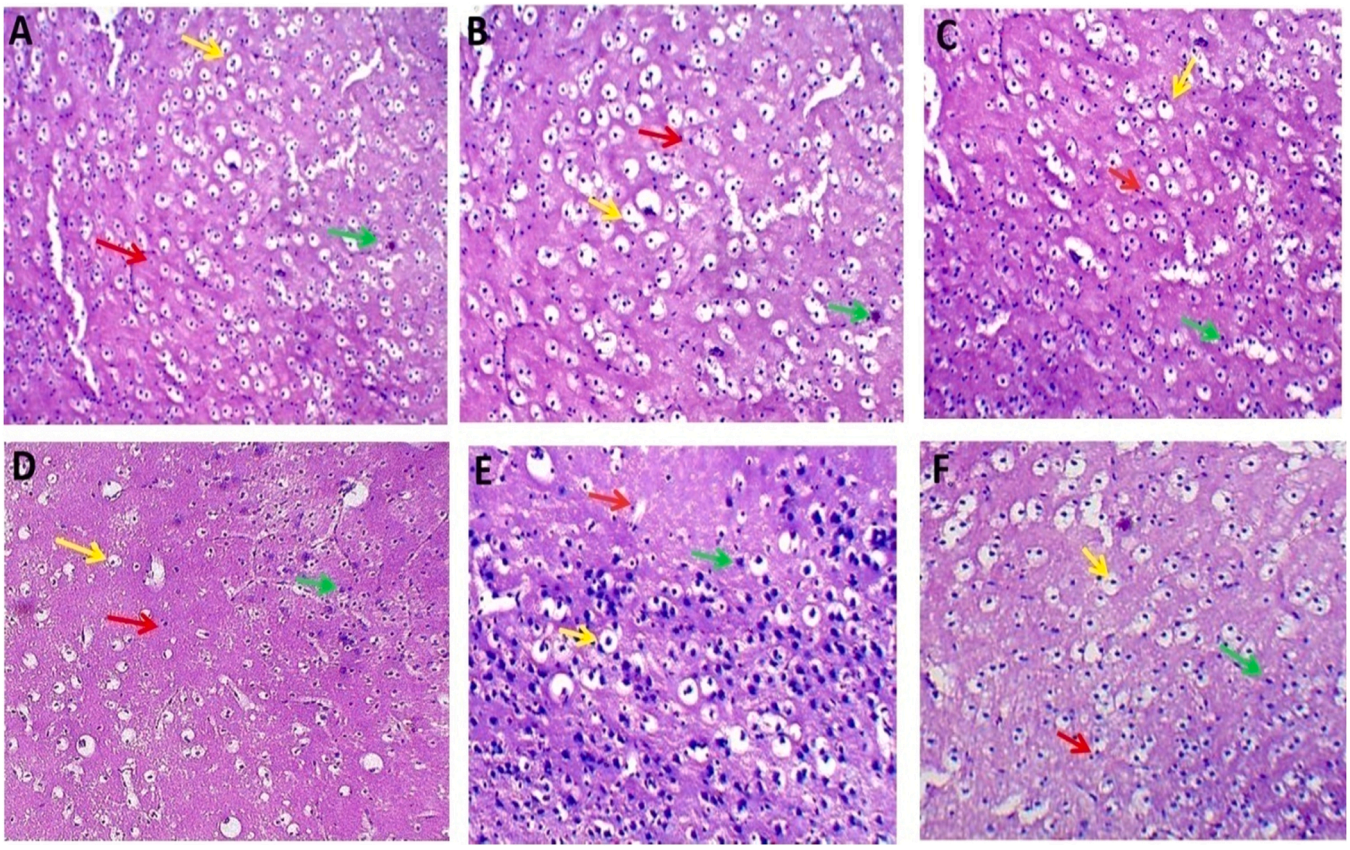

Fig. 18. Neuroprotective effect of α-mangostin in methylmercury-induced histopathological changes in experimental rats. The Panel in the figure represents neuronal populations stained with Hematoxylin and eosin under a fluorescence microscope. Light microphotographs showed the following morphological alterations in the cerebral cortex during $MeHg^{+}$ exposure and AMG treatment. 'Section: A' represents the vehicle group. The yellow arrow represents healthy oligodendrocytes cells, mainly present in the cerebral cortex. The red arrow denotes normal-appearing astrocytes. The green arrow shows microglial cells. 'Section: B' represents the sham control group, with yellow arrows representing healthy oligodendrocyte cells, red arrows representing clear and well-structured astrocytes, and green arrows representing optimum microglial cells. 'Section: C' represents the AMG perse treated group showing all neuronal cells' normal patterns like the sham control group. 'Section: D' shows a $MeHg^{+}$ treated group indicating degeneration of oligodendrocytes and astrocytes as shown by the yellow and red arrows, an increase in the density of microglial (green arrow). 'Section: E' represents $MeHg^{+}$ and AMG (100 mg/kg) treated group show a regeneration of oligodendrocyte represented by the yellow arrow, decrease in the density of microglial cells shown by the green arrow, the red arrow shows an increase in astrocytes. 'Section: F' represents $MeHg^{+}$ and AMG (200 mg/kg) treated group showed the improved structure of astrocyte represented by the red arrow, restoration of healthy oligodendrocyte by the yellow arrow, and reduced microglial density by the green arrow.

reduced TNF- and IL-1 levels in biological samples. An imbalance of oxidants and antioxidants in a biological system causes oxidative stress, which can be triggered by an excess of reactive oxygen species (ROS) or a loss in antioxidant system functioning [135]. Multiple studies in mice have connected higher ROS generation to MeHg+ exposure and MeHg+ -induced oxidative damage in the presence of MeHg+. The binding of MeHg+ to particular thiol-containing proteins may cause oxidative stress and mitochondrial membrane loss, contributing to the pathogenesis of MND [136,137].

The neuroprotective and antioxidant effects of AMG were investigated in MeHg+ -induced experimental rats. When rats were subjected to ALS-like stimuli, cellular oxidative indicators such as AchE, LDH, MDA, and nitrite increased substantially. In contrast, antioxidants such as SOD and GSH levels were significantly declined. Chronic AMG treatment markedly lowered oxidative stress marker concentrations in whole brain homogenates while raising antioxidant levels. However, this study implies that AMG may perform an antioxidant effect in reducing the incidence of oxidative stress. Furthermore, AMG exhibited neuroprotective benefits against MeHg+ -induced gross morphological and pathological changes in rat whole brain and brain slices. According to our current findings, AMG treatment significantly restored extensive morphological deficits throughout the brain and reduced pathogenic variations in specific brain regions.

Furthermore, AMG affected the amount of MBP in damaged neurons. Similarly, AMG demonstrated significant dose-dependent increases in myelin regeneration and decreased demyelination volume. These findings suggest that continuous AMG treatment may be a viable option for treating neurodegenerative symptoms associated with demyelinating illnesses like ALS [138,139].

Previous research has found that the intactness and prominent morphology of Oligodendrocytes [138,140,141], Astrocytes [142,143], and microglial cells [144] in ALS patients have been altered. Our results indicate that AMG protects against MeHg+ -induced neurotoxicity in the cerebral cortex of rats. According to our current findings, when AMG was administered at doses of 100 mg/kg and 200 mg/kg, the density of neuroglial cells was restored. However, histology demonstrated that structural integrity had been lost in the MeHg+ treated group. AMG treatment at 100 mg/kg and 200 mg/kg doses also recovered neuroglial cells. The study findings associated with AMG, on the other hand, were principally investigated to alleviate neurobehavioral and neurochemical deficits in MeHg+ -treated rats via altering ERK-1/2 signalling. Our results show that ERK-1/2 and MBP levels in brain tissue, blood plasma, and cerebrospinal fluid (CSF) could be employed as an early diagnostic biomarker for identifying an important degenerative feature of ALS brain. While ERK-1/2 levels in CSF increase by 12.5 times in MeHg+ -treated rats compared to normal control rats, they remain 7.76 times

higher in alpha-mangostin-treated rats. This highlights the crucial need for more effective therapeutic agents, which we intend to investigate further.

5.1. Limitations

The ERK cascade is essential for cell proliferation, differentiation, adhesion, migration, and survival. As a result, it participates in a variety of physiological processes. Qualitative investigations of cellular markers such as Western blotting and immunohistopathology would be required to establish the molecular basis for this approach. Given these limitations, AMG's ability to restore or downregulate ERK-1/2 signalling pathways in the brain may aid in the development of a potential therapeutic strategy for this neurodegenerative condition.

6. Conclusion

In this study, MeHg+ -induced rats show severe cognitive impairment, memory loss, motor impairments, ERK-1/2 upregulation, and neuronal cell death. Our findings show that oral administration of AMG at doses of 100 mg/kg and 200 mg/kg alleviates the neurobehavioral and neuropathological changes caused by MeHg+ injection and reduces ERK-1/2 levels in the rat brain. There have been no follow-up investigations on AMG's neuroprotective benefits via ERK-1/2 signalling in MeHg+ -induced rats. As a result of these findings, we suggest that AMG could be a viable therapy option for alleviating the various behavioural, biochemical, neurochemical, and morphological alterations associated with the development and progression of MeHg+ -treated rats. We also measured neurochemical levels in rat brain homogenate, cerebrospinal fluid (CSF), and blood plasma. Our findings suggest that AMG is an important phytochemical that reverses biochemical abnormalities in the rat brain and MBP levels in MeHg+ -induced rats via inhibiting the ERK-1/2 signalling pathway.

Furthermore, AMG reversed significant morphological and gross pathogenic abnormalities in MeHg+ -induced rat's whole brain and brain sections. Based on our histology findings, we may conclude that MeHg+ is a neurotoxin harmful to neuroglial cells. In the cerebral cortical sections of the rat brain, MeHg+ -induced ALS is characterised by the death of oligodendrocytes and an increase in the density of microglial and astrocyte cells. AMG therapy at doses of 100 mg/kg and 200 mg/kg reduces MeHg+ toxicity and restores oligodendrocyte, microglia, and astrocyte structural integrity. Finally, AMG could be a new pharmacological approach for treating neurological dysfunction, involving alterations in various neurochemical pathways. However, further research is needed to determine the level of ERK-1/2 in ALS utilising western blot, RT-PCR, immunohistopathology, and genetic encoding and evaluate the efficacy of AMG in ALS.

Funding

This work was supported by institutional grants from the Institutional Animal Ethics Committee (IAEC) with registration no. 816/PO/ReBiBt/S/04/CPCSEA as protocol no. ISFCP/IAEC/CPCSEA/Meeting No.28/2020/Protocol No.464 approved by RAB Committee, ISFCP, Moga, Punjab, India.

CRediT authorship contribution statement

Investigation, Original Draft, Writing review, R.S., A.P. S.K; Formal analysis, Data curation, Validation, Editing A.P., A.A., M.A, M.A.A.; Conceptualisation, Resources, Supervision, S.M, A.S.N.All data were generated in-house, and no paper mill was used. All authors agree to be accountable for all aspects of work, ensuring integrity and accuracy. All authors read and approved the manuscript and all data were generated in-house and that no paper mill was used.

Declaration of Competing Interest

The authors declare that they have no known competing financial interests or personal relationships that could have appeared to influence the work reported in this paper.

Data availability

All data generated or analysed during this study are included in this article. There are no separate or additional files.

Acknowledgements

The authors express their gratitude to the Chairman, Mr. Parveen Garg, and Director, Dr. G.D. Gupta, ISF College of Pharmacy, Moga, Punjab, India, for their extraordinary vision and overwhelming support. The authors are also thankful to the Researchers Supporting Project number (RSP2022R491), King Saud University, Riyadh, Saudi Arabia.

Appendix A. Supporting information

Supplementary data associated with this article can be found in the online version at doi:10.1016/j.toxrep.2022.04.023.

References

[1] E.M. Nolan, S.J. Lippard, Tools and tactics for the optical detection of mercuric ion, Chem. Rev. 108 (9) (2008) 3443–3480.
[2] A. Colón-Rodríguez, H.E. Hannon, W.D. Atchison, Effects of methylmercury on spinal cord afferents and efferents – a review, Neurotoxicology 60 (2017) 308–320.
[3] T.W. Clarkson, L. Magos, G.J. Myers, The toxicology of mercury – current exposures and clinical manifestations, N. Engl. J. Med. 349 (18) (2003) 1731–1737.
[4] A.F. Castoldi, C. Johansson, N. Onishchenko, T. Coccini, E. Roda, M. Vahter, S. Ceccatelli, L. Manzo, Human developmental neurotoxicity of methylmercury: impact of variables and risk modifiers, Regul. Toxicol. Pharmacol. 51 (2) (2008) 201–214.
[5] Rajeshwar Kumar Yadav, et al., Protective effects of apigenin on methylmercury-induced behavioral/neurochemical abnormalities and neurotoxicity in rats, Hum. Exp. Toxicol. 41 (2022), https://doi.org/10.1177/09603271221084276.
[6] M. Alam, R.K. Yadav, E. Minj, A. Tiwari, S. Mehan, Exploring molecular approaches in amyotrophic lateral sclerosis: drug targets from clinical and preclinical findings, Curr. Mol. Pharmacol. (2020), https://doi.org/10.2174/1566524020666200427214356.
[7] E. Minj, S. Upadhayay, S. Mehan, Nrf2/HO-1 signaling activator acetyl-11-keto-beta boswellic acid (AKBA)-mediated neuroprotection in methyl mercury-induced experimental model of ALS, Neurochem. Res. 46 (11) (2021) 2867–2884, https://doi.org/10.1007/s11064-021-03366-2.
[8] T.H. Lu, S.Y. Hsieh, C.C. Yen, H.C. Wu, K.L. Chen, D.Z. Hung, C.H. Chen, C.C. Wu, Y.C. Su, Y.W. Chen, S.H. Liu, C.F. Huang, Involvement of oxidative stress-mediated ERK1/2 and p38 activation regulated mitochondria-dependent apoptotic signals in methylmercury-induced neuronal cell injury, Toxicol. Lett. 204 (1) (2011) 71–80, https://doi.org/10.1016/j.toxlet.2011.04.013.
[9] J.A. Parkin Kullmann, R. Pamphlett, A comparison of mercury exposure from seafood consumption and dental amalgam fillings in people with and without amyotrophic lateral sclerosis (ALS): an international online case-control study, Int J. Environ. Res Public Health 15 (12) (2018) 2874, https://doi.org/10.3390/ijerph15122874. PMID: 30558238; PMCID: PMC6313312.
[10] R. Pamphlett, S. Kum Jew, Uptake of inorganic mercury by human locus ceruleus and corticomotor neurons: implications for amyotrophic lateral sclerosis, Acta Neuropathol. Commun. 1 (13) (2013), https://doi.org/10.1186/2051-5960-1-13 (PMID: 24252585; PMCID: PMC3893560).
[11] P.E. Ash, U. Dhawan, S. Boudeau, S. Lei, Y. Carlomagno, M. Knobel, L.F. Al Mohanna, S.R. Boomhower, M.C. Newland, D.H. Sherr, B. Wolozin, Heavy metal neurotoxicants induce ALS-linked TDP-43 pathology, Toxicol. Sci. 167 (1) (2019) 105–115.
[12] A. Prasad, V. Bharathi, V. Sivalingam, A. Girdhar, B.K. Patel, Molecular mechanisms of TDP-43 misfolding and pathology in amyotrophic lateral sclerosis, Front. Mol. Neurosci. 12 (2019) 25.
[13] P. Masrori, P. Van Damme, Amyotrophic lateral sclerosis: a clinical review, Eur. J. Neurol. 27 (10) (2020) 1918–1929, https://doi.org/10.1111/ene.14393. Epub 2020 Jul 7. PMID: 32526057; PMCID: PMC7540334.
[14] R.K. Yadav, E. Minj, S. Mehan, Understanding correlation of abnormal c-JNK/p38MAPK signaling in amyotrophic lateral sclerosis: potential drug targets and influences on neurological disorders, CNS Neurol. Disord. Drug Targets (2021), https://doi.org/10.2174/1871527320666210126113848. Epub ahead of print. PMID: 33557726.

[15] S. Dhasmana, A. Dhasmana, A.S. Narula, M. Jaggi, M.M. Yallapu, S.C. Chauhan, The panoramic view of amyotrophic lateral sclerosis: a fatal intricate neurological disorder, Life Sci. 288 (2022), 120156.
[16] K. Abhinav, B. Stanton, C. Johnston, J. Hardstaff, R.W. Orrell, R. Howard, J. Clarke, M. Sakel, M.A. Ampong, C.E. Shaw, P.N. Leigh, A. Al-Chalabi, Amyotrophic lateral sclerosis in South-East England: a population-based study. The South-East England register for amyotrophic lateral sclerosis (SEALS Registry), Neuroepidemiology 29 (1–2) (2007) 44–48, https://doi.org/10.1159/000108917. Epub 2007 Sep 24.
[17] J.M. Bailey, A. Colón-Rodríguez, W.D. Atchison, Evaluating a gene-environment interaction in amyotrophic lateral sclerosis: methylmercury exposure and mutated SOD1, Curr. Environ. Health Rep. 4 (2) (2017) 200–207.
[18] L. Koski, C. Ronnevi, E. Berntsson, S.K. Wärmländer, P.M. Roos, Metals in ALS TDP-43 pathology, Int. J. Mol. Sci. 22 (22) (2021) 12193.
[19] T.J. Cohen, A.W. Hwang, C.R. Restrepo, C.X. Yuan, J.Q. Trojanowski, V.M. Lee, An acetylation switch controls TDP-43 function and aggregation propensity, Nat. Commun. 6 (1) (2015) 1–3.
[20] M. Sabatelli, M. Zollino, A. Conte, A. Del Grande, G. Marangi, M. Lucchini, M. Mirabella, A. Romano, R. Piacentini, G. Bisogni, S. Lattante, M. Luigetti, P. M. Rossini, A. Moncada, Primary fibroblasts cultures reveal TDP-43 abnormalities in amyotrophic lateral sclerosis patients with and without SOD1 mutations, Neurobiol. Aging 36 (5) (2015) 2005, https://doi.org/10.1016/j.neurobiolaging.2015.02.009. Epub 2015 Feb 17.
[21] Y.H. Chung, K.M. Joo, H.C. Lim, M.H. Cho, D. Kim, W.B. Lee, C.I. Cha, Immunohistochemical study on the distribution of phosphorylated extracellular signal-regulated kinase (ERK) in the central nervous system of SOD1G93A transgenic mice, Brain Res. 1050 (1–2) (2005) 203–209, https://doi.org/10.1016/j.brainres.2005.05.060.
[22] V. Ayala, A.B. Granado-Serrano, D. Cacabelos, A. Naudí, E.V. Ilieva, J. Boada, V. Caraballo-Miralles, J. Lladó, I. Ferrer, R. Pamplona, M. Portero-Otin, Cell stress induces TDP-43 pathological changes associated with ERK1/2 dysfunction: implications in ALS, Acta Neuropathol. 122 (3) (2011) 259–270, https://doi.org/10.1007/s00401-011-0850-y.
[23] W. Wang, D. Wen, W. Duan, J. Yin, C. Cui, Y. Wang, Z. Li, Y. Liu, C. Li, Systemic administration of scAAV9-IGF1 extends survival in SOD1G93A ALS mice via inhibiting p38 MAPK and the JNK-mediated apoptosis pathway, Brain Res. Bull. 139 (2018) 203–210, https://doi.org/10.1016/j.brainresbull.2018.02.015.
[24] R. Sahu, S. Upadhayay, S. Mehan, Inhibition of extracellular regulated kinase (ERK)-1/2 signaling pathway in the prevention of ALS: target inhibitors and influences on neurological dysfunctions, Eur. J. Cell Biol. 100 (7–8) (2021), 151179.
[25] M.C. Harrisingh, E. Perez-Nadales, D.B. Parkinson, D.S. Malcolm, A.W. Mudge, A. C. Lloyd, The Ras/Raf/ERK signalling pathway drives Schwann cell dedifferentiation, EMBO J. 23 (15) (2004) 3061–3071, https://doi.org/10.1038/sj.emboj.7600309.
[26] T. Ogata, S. Iijima, S. Hoshikawa, T. Miura, S. Yamamoto, H. Oda, K. Nakamura, S. Tanaka, Opposing extracellular signal-regulated kinase and Akt pathways control Schwann cell myelination, J. Neurosci. 24 (30) (2004) 6724–6732, https://doi.org/10.1523/JNEUROSCI.5520-03.2004.
[27] I. Napoli, L.A. Noon, S. Ribeiro, A.P. Kerai, S. Parrinello, L.H. Rosenberg, M. J. Collins, M.C. Harrisingh, I.J. White, A. Woodhoo, A.C. Lloyd, A central role for the ERK-signaling pathway in controlling Schwann cell plasticity and peripheral nerve regeneration in vivo, Neuron 73 (4) (2012) 729–742, https://doi.org/10.1016/j.neuron.2011.11.031.
[28] N. Suo, Y.E. Guo, B. He, H. Gu, X. Xie, Inhibition of MAPK/ERK pathway promotes oligodendrocytes generation and recovery of demyelinating diseases, Glia 67 (7) (2019) 1320–1332, https://doi.org/10.1002/glia.23606.
[29] M. Redza-Dutordoir, D.A. Averill-Bates, Activation of apoptosis signalling pathways by reactive oxygen species, Biochim. Biophys. Acta (BBA)-Mol. Cell Res. 1863 (12) (2016) 2977–2992, https://doi.org/10.1016/j.bbamcr.2016.09.012.
[30] S.H. Kim, C.J. Smith, L.J. Van Eldik, Importance of MAPK pathways for microglial pro-inflammatory cytokine IL-1β production, Neurobiol. Aging 25 (4) (2004) 431–439, https://doi.org/10.1016/s0197-4580(03)00126-x.
[31] H.T. Liu, Y.G. Du, J.L. He, W.J. Chen, W.M. Li, Z. Yang, Y.X. Wang, C. Yu, Tetramethylpyrazine inhibits production of nitric oxide and inducible nitric oxide synthase in lipopolysaccharide-induced N9 microglial cells through blockade of MAPK and PI3K/Akt signaling pathways, and suppression of intracellular reactive oxygen species, J. Ethnopharmacol. 129 (3) (2010) 335–343, https://doi.org/10.1016/j.jep.2010.03.037.
[32] S.W. Himaya, B. Ryu, Z.J. Qian, Y. Li, S.K. Kim, 1-(5-bromo-2-hydroxy-4-methoxyphenyl) ethanone [SE1] suppresses pro-inflammatory responses by blocking NF-κB and MAPK signaling pathways in activated microglia, Eur. J. Pharmacol. 670 (2–3) (2011) 608–616, https://doi.org/10.1016/j.ejphar.2011.09.013.
[33] X. Su, Q. Chen, W. Chen, T. Chen, W. Li, Y. Li, X. Dou, Y. Zhang, Y. Shen, H. Wu, C. Yu, Mycoepoxydiene inhibits activation of BV2 microglia stimulated by lipopolysaccharide through suppressing NF-κB, ERK 1/2 and toll-like receptor pathways, Int. Immunopharmacol. 19 (1) (2014) 88–93, https://doi.org/10.1016/j.intimp.2014.01.004.
[34] S.M. Kulich, C.T. Chu, Sustained extracellular signal-regulated kinase activation by 6-hydroxydopamine: implications for Parkinson's disease, J. Neurochem 77 (4) (2001) 1058–1066, https://doi.org/10.1046/j.1471-4159.2001.00304.x.
[35] C. Russo, V. Dolcini, S. Salis, V. Venezia, N. Zambrano, T. Russo, G. Schettini, Signal transduction through tyrosine-phosphorylated C-terminal fragments of amyloid precursor protein via an enhanced interaction with Shc/Grb2 adaptor proteins in reactive astrocytes of Alzheimer's disease brain, J. Biol. Chem. 277 (38) (2002) 35282–35288, https://doi.org/10.1074/jbc.m110785200.
[36] S. Sheikh, Safia, E. Haque, S.S. Mir, Neurodegenerative diseases: multifactorial conformational diseases and their therapeutic interventions, J. Neurodegener. Dis. 2013 (2013), 563481, https://doi.org/10.1155/2013/563481.
[37] T. Sugino, K. Nozaki, Y. Takagi, I. Hattori, N. Hashimoto, T. Moriguchi, E. Nishida, Activation of mitogen-activated protein kinases after transient forebrain ischemia in gerbil hippocampus, J. Neurosci. 20 (12) (2000) 4506–4514, https://doi.org/10.1523/jneurosci.20-12-04506.2000.
[38] E.K. Kim, E.J. Choi, Pathological roles of MAPK signaling pathways in human diseases, Biochim. Acta 1802 (4) (2010) 396–405, https://doi.org/10.1016/j.bbadis.2009.12.009. Epub 2010 Jan 14.
[39] J. Sun, G. Nan, The extracellular signal-regulated kinase 1/2 pathway in neurological diseases: a potential therapeutic target (Review), Int J. Mol. Med 39 (6) (2017) 1338–1346, https://doi.org/10.3892/ijmm.2017.2962.
[40] T.H. Lu, S.Y. Hsieh, C.C. Yen, H.C. Wu, K.L. Chen, D.Z. Hung, C.H. Chen, C.C. Wu, Y.C. Su, Y.W. Chen, S.H. Liu, C.F. Huang, Involvement of oxidative stress-mediated ERK1/2 and p38 activation regulated mitochondria-dependent apoptotic signals in methylmercury-induced neuronal cell injury, Toxicol. Lett. 204 (1) (2011) 71–80, https://doi.org/10.1016/j.toxlet.2011.04.013.
[41] K. Zhang, Q. Liu, D. Shen, H. Tai, S. Liu, Z. Wang, J. Shi, H. Fu, S. Wu, Q. Ding, Y. Hu, Mutation analysis of KIF5A in Chinese amyotrophic lateral sclerosis patients, Neurobiol. Aging 73 (2019) 229–e1, https://doi.org/10.1016/j.neurobiolaging.2018.08.006.
[42] Z.Q. Wang, D.C. Wu, F.P. Huang, G.Y. Yang, Inhibition of MEK/ERK 1/2 pathway reduces pro-inflammatory cytokine interleukin-1 expression in focal cerebral ischemia, Brain Res. 996 (1) (2004) 55–66, https://doi.org/10.1016/j.brainres.2003.09.074.
[43] D. Ortuno-Sahagún, R.M. González, E. Verdaguer, V.C. Huerta, B.M. Torres-Mendoza, L. Lemus, M.C. Rivera-Cervantes, A. Camins, C.B. Zárate, Glutamate excitotoxicity activates the MAPK/ERK signaling pathway and induces the survival of rat hippocampal neurons in vivo, J. Mol. Neurosci. 52 (3) (2014) 366–377, https://doi.org/10.1007/s12031-013-0157-7.
[44] M. Cargnello, P.P. Roux, Activation and function of the MAPKs and their substrates, the MAPK-activated protein kinases, Microbiol. Mol. Biol. Rev. 75 (1) (2011) 50–83, https://doi.org/10.1128/mmbr.00031-10.
[45] P.K. Wu, J.I. Park, MEK1/2 inhibitors: molecular activity and resistance mechanisms, Semin. Oncol. 42 (2015) 849–862, https://doi.org/10.1053/j.seminoncol.2015.09.023.
[46] C. Fremin, S. Meloche, From basic research to clinical development of MEK1/2 inhibitors for cancer therapy, J. Hematol. Oncol. 3 (1) (2010), https://doi.org/10.1186/1756-8722-3-8.
[47] S.D. Barrett, A.J. Bridges, D.T. Dudley, A.R. Saltiel, J.H. Fergus, C.M. Flamme, A. M. Delaney, M. Kaufman, S. LePage, W.R. Leopold, S.A. Przybranowski, The discovery of the benzhydroxamate MEK inhibitors CI-1040 and PD 0325901, Bioorg. Med. Chem. Lett. 18 (24) (2008) 6501–6504, https://doi.org/10.1016/j.bmcl.2008.10.054.
[48] A. Banerjee, R.I. Jakacki, A. Onar-Thomas, S. Wu, T. Nicolaides, T. Young Poussaint, J. Fangusaro, J. Phillips, A. Perry, D. Turner, M. Prados, A phase I trial of the MEK inhibitor selumetinib (AZD6244) in pediatric patients with recurrent or refractory low-grade glioma: a pediatric brain tumor consortium (PBTC) study, Neuro-Oncology 19 (8) (2017) 1135–1144, https://doi.org/10.1093/neuonc/now282.
[49] C.E. Le Pichon, S.L. Dominguez, H. Solanoy, H. Ngu, N. Lewin-Koh, M. Chen, J. Eastham-Anderson, R. Watts, K. Scearce-Levie, EGFR inhibitor erlotinib delays disease progression but does not extend survival in the SOD1 mouse model of ALS, PLOS One 8 (4) (2013), e62342, https://doi.org/10.1371/journal.pone.0062342.
[50] H. Blasco, S. Mavel, P. Corcia, P.H. Gordon, The glutamate hypothesis in ALS: pathophysiology and drug development, Curr. Med. Chem. 21 (31) (2014) 3551–3575, https://doi.org/10.2174/0929867321666140916120118.
[51] S. Mignani, J.P. Majoral, J.F. Desaphy, G. Lentini, From riluzole to dexpramipexole via substituted-benzothiazole derivatives for amyotrophic lateral sclerosis disease treatment: case studies, Molecules 25 (15) (2020) 3320, https://doi.org/10.3390/molecules25153320.
[52] K. Abe, M. Aoki, S. Tsuji, Y. Itoyama, G. Sobue, M. Togo, C. Hamada, M. Tanaka, M. Akimoto, K. Nakamura, F. Takahashi, Safety and efficacy of edaravone in well defined patients with amyotrophic lateral sclerosis: a randomised, double-blind, placebo-controlled trial, Lancet Neurol. 16 (7) (2017) 505–512, https://doi.org/10.1016/s1474-4422(17)30115-1.
[53] J.S. Mora, Edaravone for treatment of early-stage ALS, Lancet Neurol. 16 (10) (2017) 772, https://doi.org/10.1016/s1474-4422(17)30289-2.
[54] P. Janhom, P. Dharmasaroja, Neuroprotective effects of alpha-mangostin on MPP(+)-induced apoptotic cell death in neuroblastoma SH-SY5Y cells, J. Toxicol. 2015 (2015), 919058, https://doi.org/10.1155/2015/919058. Epub 2015 Aug 18. PMID: 26357513; PMCID: PMC4556078.
[55] D.R. Herrera-Aco, O.N. Medina-Campos, J. Pedraza-Chaverri, E. Sciutto-Conde, G. Rosas-Salgado, G. Fragoso-González, Alpha-mangostin: anti-inflammatory and antioxidant effects on established collagen-induced arthritis in DBA/1J mice, Food Chem. Toxicol. 124 (2019) 300–315, https://doi.org/10.1016/j.fct.2018.12.018. Epub 2018 Dec 14.
[56] F. Gutierrez-Orozco, C. Chitchumroonchokchai, G.B. Lesinski, S. Suksamrarn, M. L. Failla, α-Mangostin: anti-inflammatory activity and metabolism by human cells, J. Agric. Food Chem. 61 (16) (2013) 3891–3900, https://doi.org/10.1021/jf4004434. Epub 2013 Apr 11. PMID: 23578285; PMCID: PMC3793015.

[57] M. Sivaranjani, M. Prakash, S. Gowrishankar, J. Rathna, S.K. Pandian, A.V. Ravi, In vitro activity of alpha-mangostin in killing and eradicating Staphylococcus epidermidis RP62A biofilms, Appl. Microbiol. Biotechnol. 101 (8) (2017) 3349–3359, https://doi.org/10.1007/s00253-017-8231-7. Epub 2017 Mar 25.
[58] A. Tiwari, R. Khera, S. Rahi, S.* Mehan, H.A. Makeen, Y.H. Khormi, M. U. Rehman, A. Khan, Neuroprotective effect of α-mangostin in the ameliorating propionic acid-induced experimental model of autism in wistar rats, Brain Sci. 11 (3) (2021) 288, https://doi.org/10.3390/brainsci11030288. PMID: 33669120; PMCID: PMC7996534.
[59] W. Weecharangsan, P. Opanasopit, M. Sukma, T. Ngawhirunpat, U. Sotanaphun, P. Siripong, Antioxidative and neuroprotective activities of extracts from the fruit hull of mangosteen (Garcinia mangostana Linn.), Med. Princ. Pract. 15 (4) (2006) 281–287, https://doi.org/10.1159/000092991.
[60] N. Dey, B. Leyland-Jones, P. De, MYC-xing it up with PIK3CA mutation and resistance to PI3K inhibitors: summit of two giants in breast cancers, Am. J. Cancer Res. 5 (1) (2014) 1–19. PMID: 25628917; PMCID: PMC4300701.
[61] J. Sattayasai, P. Chaonapan, T. Arkaravichie, R. Soi-Ampornkul, S. Junnu, P. Charoensilp, J. Samer, J. Jantaravinid, P. Masaratana, B. Suktitipat, J. Manissorn, V. Thongboonkerd, N. Neungton, P. Moongkarndi, Protective effects of mangosteen extract on H2O2-induced cytotoxicity in SK-N-SH cells and scopolamine-induced memory impairment in mice, PLOS One 8 (12) (2013), e85053, https://doi.org/10.1371/journal.pone.0085053. PMID: 24386444; PMCID: PMC3874002.
[62] B. Harvey, I. Oberholzer, J. Lotter, M. Möller, B. Holland, O. Dean, M. Berk, Garcinia mangostana Linn displays antidepressant, antipsychotic and procognitive effects in translational models of depression and schizophrenia: role of serotonin and immune-inflammatory cascades. Proceedings of the 19th Congress of the International Serotonin Society, University College Cork,, Cork, 2018, pp. 15–19.
[63] A. Plotnikov, D. Chuderland, Y. Karamansha, O. Livnah, R. Seger, Nuclear extracellular signal-regulated kinase 1 and 2 translocation is mediated by casein kinase 2 and accelerated by autophosphorylation, Mol. Cell. Biol. 31 (17) (2011) 3515–3530, https://doi.org/10.1128/mcb.05424-11.
[64] J. Christinal, T. Sumathi, Effect of Bacopa monniera extract on methylmercuryinducedbehavioral and histopathological changes in rats, Biol. Trace Elem. 155 (1) (2013) 56–64, https://doi.org/10.1007/s12011-013-9756-y.
[65] S.A. Bailey, R.H. Zidell, R.W. Perry, Relationships between organ weight and body/brain weight in the rat: what is the best analytical endpoint? Toxicol. Pathol. 32 (4) (2004) 448–466, https://doi.org/10.1080/01926230490465874.
[66] R. Morris, Developments of a water-maze procedure for studying spatial learning in the rat, J. Neurosci. Methods 11 (1) (1984) 47–60, https://doi.org/10.1016/0165-0270(84)90007-4.
[67] P. Duggal, K.S. Jadaun, E.M. Siqqiqui, S. Mehan, Investigation of low dose cabazitaxel potential as microtubule stabilizer in experimental model of alzheimer's disease: restoring neuronal cytoskeleton, Curr. Alzheimer Res. 17 (7) (2020) 601–615, https://doi.org/10.2174/1567205017666201007120112.
[68] S.* Mehan, S. Rahi, A. Tiwari, T. Kapoor, K. Rajdev, R. Sharma, H. Khera, S. Kosey, U. Kukkar, R. Dudi, Adenylate cyclase activator forskolin alleviates intracerebroventricular propionic acid-induced mitochondrial dysfunction of autistic rats, Neural Regen. Res. 15 (6) (2020) 1140–1149, https://doi.org/10.4103/1673-5374.270316. PMID: 31823895; PMCID: PMC7034277.
[69] S.* Mehan, V. Monga, M. Rani, R. Dudi, K. Ghimire, Neuroprotective effect of solanesol against 3-nitropropionic acid-induced Huntington's disease-like behavioral, biochemical, and cellular alterations: restoration of coenzyme-Q10-mediated mitochondrial dysfunction, Indian J. Pharm. 50 (6) (2018) 309–319, https://doi.org/10.4103/ijp.IJP_11_18. PMID: 30783323; PMCID: PMC6364342.
[70] R. Sharma, S. Rahi, S. Mehan, Neuroprotective potential of solanesol in intracerebroventricular propionic acid induced experimental model of autism: insights from behavioral and biochemical evidence, Toxicol. Rep. 6 (2019) 1164–1175, https://doi.org/10.1016/j.toxrep.2019.10.019. PMID: 31763180; PMCID: PMC6861559.
[71] R. Khera, S. Mehan, S. Bhalla, S. Kumar, A. Alshammari, M. Alharbi, S.S. Sadhu, Guggulsterone mediated JAK/STAT and PPAR-gamma modulation prevents neurobehavioral and neurochemical abnormalities in propionic acid-induced experimental model of autism, Molecules 27 (3) (2022) 889.
[72] C.C. Pegg, C. He, A.R. Stroink, K.A. Kattner, C.X. Wang, Technique for collection of cerebrospinal fluid from the cisterna magna in rat, J. Neurosci. Methods 187 (1) (2010) 8–12, https://doi.org/10.1016/j.jneumeth.2009.12.002. Epub 2009 Dec 11.
[73] R. Nirogi, V. Kandikere, K. Mudigonda, G. Bhyrapuneni, N. Muddana, R. Saralaya, V. Benade, A simple and rapid method to collect the cerebrospinal fluid of rats and its application for the assessment of drug penetration into the central nervous system, J. Neurosci. Methods 178 (1) (2009) 116–119, https://doi.org/10.1016/j.jneumeth.2008.12.001. Epub 2008 Dec 6.
[74] K. Duris, A. Manaenko, H. Suzuki, W. Rolland, J. Tang, J.H. Zhang, Sampling of CSF via the cisterna magna and blood collection via the heart affects brain water content in a rat SAH model, Transl. Stroke Res. 2 (2) (2011) 232–237, https://doi.org/10.1007/s12975-010-0063-z. PMID: 21666823; PMCID: PMC3109988.
[75] S. Mehan, S. Parveen, S. Kalra, Adenyl cyclase activator forskolin protects against Huntington's disease-like neurodegenerative disorders, Neural Regen. Res. 12 (2) (2017) 290–300, https://doi.org/10.4103/1673-5374.200812. PMID: 28400813; PMCID: PMC5361515.
[76] S. Mahinrad, M. Bulk, I. van der Velpen, A. Mahfouz, W. van Roon-Mom, N. Fedarko, S. Yasar, B. Sabayan, D. van Heemst, L. van der Weerd, Natriuretic peptides in post-mortem brain tissue and cerebrospinal fluid of non-demented humans and alzheimer's disease patients, Front. Neurosci. 12 (2018) 864, https://doi.org/10.3389/fnins.2018.00864. PMID: 30534047; PMCID: PMC6275179.
[77] N. Kumar, N. Sharma, R. Khera, R. Gupta, S.* Mehan, Guggulsterone ameliorates ethidium bromide-induced experimental model of multiple sclerosis via restoration of behavioral, molecular, neurochemical and morphological alterations in rat brain, Metab. Brain Dis. 36 (5) (2021) 911–925, https://doi.org/10.1007/s11011-021-00691-x. Epub 2021 Feb 26.
[78] K.S. Jadaun, S. Mehan, A. Sharma, E.M. Siddiqui, S. Kumar, N. Alsuhaymi, Neuroprotective effect of chrysophanol as a PI3K/AKT/mTOR signaling inhibitor in an experimental model of autologous blood-induced intracerebral hemorrhage, Curr. Med. Sci. (2022) 1–8.
[79] M. Bai, B. Liu, M. Peng, J. Jia, X. Fang, M. Miao, Effect of sargentodoxacuneata total phenolic acids on focal cerebral ischemia reperfusion injury rats model, Saudi J. Biol. Sci. 26 (3) (2019) 569–576, https://doi.org/10.1016/j.sjbs.2018.11.019.
[80] S. Rahi, R. Gupta, A. Sharma, S.* Mehan, Smo-Shh signaling activator purmorphamine ameliorates neurobehavioral, molecular, and morphological alterations in an intracerebroventricular propionic acid-induced experimental model of autism, Hum. Exp. Toxicol. (2021), 9603271211013456. doi: 10.1177/09603271211013456. Epub ahead of print. PMID: 33906504.
[81] R. Verma, R. Bhatia, G. Singh, B. Kumar, S. Mehan, V. Monga, Design, synthesis and neuropharmacological evaluation of new 2,4-disubstituted-1,5-benzodiazepines as CNS active agents, Bioorg. Chem. 101 (2020), 104010, https://doi.org/10.1016/j.bioorg.2020.104010. Epub 2020 Jun 16.
[82] K. Rajdev, E.M. Siddiqui, K.S. Jadaun, S. Mehan, Neuroprotective potential of solanesol in a combined model of intracerebral and intraventricular hemorrhage in rats, IBRO Rep. 8 (2020) 101–114, https://doi.org/10.1016/j.ibror.2020.03.001. PMID: 32368686; PMCID: PMC7184235.
[83] S. Mehan, A. Verma, K. Bedi, V. Sehgal, H. Meena, D. Sharma, Effect of mitogen activated protein kinase inhibitor in animal model of alzheimer's diseases, Int. J. Pharma Professional's Res. 2 (1) (2011) 177–188. ⟨http://www.ijppronline.in/index.php/IJPPR/article/view/21⟩.
[84] B.A. Patel, M. Arundell, K.H. Parker, M.S. Yeoman, D. O'Hare, Simple and rapid determination of serotonin and catecholamines in biological tissue using high-performance liquid chromatography with electrochemical detection, J. Chromatogr. B 818 (2) (2005) 269–276.
[85] R. Bala, D. Khanna, S. Mehan, S. Kalra, Experimental evidence for the potential of lycopene in the management of scopolamine induced amnesia, RSC Adv. 5 (89) (2015) 72881–72892, 10.1039/c5ra13160j; EID: 2-s2.0-84940994950.
[86] L. Singh, S. Rana, S. Mehan, Pyare L. Sharma, Role of adenylyl cyclase activator in controlling experimental diabetic nephropathy in rats, Int. J. Physiology, Pathophysiology Pharmacol. 10 (5) (2018) 144–153, https://doi.org/10.5567/pharmacologia.2014.60.75.
[87] R. Kaur, S. Mehan, Shaba Parveen, Deepa Khanna, Sanjeev kalra, Precautionary ellagic acid treatment ameliorates chronically administered scopolamine induced alzheimer's type memory and cognitive dysfunctions in rats, Pharmacologia 6 (5) (2015) 192–212, https://doi.org/10.5567/pharmacologia.2015.192.212.
[88] Dudi, R., Mehan, S., 2018. Neuroprotection of brain permeable Forskolin ameliorates behavioral, biochemical and histopathological alterations in rat model of intracerebral hemorrhage, 10(2):68-86.
[89] A. Singh, R. Kukreti, L. Saso, S. Kukreti, Oxidative Stress: A Key Modulator in Neurodegenerative Diseases, Molecules 24 (8) (2019) 1583, https://doi.org/10.3390/molecules24081583. PMID: 31013638; PMCID: PMC6514564.
[90] H. Khera, A. Awasthi, S. Mehan, Myocardial preconditioning potential of hedgehog activator purmorphamine (smoothened receptor agonist) against ischemia-reperfusion in deoxycortisone acetate salt-induced hypertensive rat hearts, J. Pharmacol. Pharmacother. 10 (2) (2019) 47.
[91] S. Rana, L. Singh, S.Forskolin Mehan, ameliorates mitochondrial dysfunction in Streptozotocin induced diabetic nephropathy in rats, Asian J. Pharm. Pharmacol. 4 (6) (2018) 744–751, 10.31024/ajpp.2019.5.1.28; Part of ISSN: 2455-2674.
[92] D. Carassiti, D.R. Altmann, N. Petrova, B. Pakkenberg, F. Scaravilli, K. Schmierer, Neuronal loss, demyelination and volume change in the multiple sclerosis neocortex, Neuropathol. Appl. Neurobiol. 44 (4) (2018) 377–390, https://doi.org/10.1111/nan.12405.
[93] V. Rajagopalan, Z. Liu, D. Allexandre, L. Zhang, X.F. Wang, E.P. Pioro, G.H. Yue, Brain white matter shape changes in amyotrophic lateral sclerosis (ALS): a fractal dimension study, PLOS One 8 (9) (2013), e73614, https://doi.org/10.1371/journal.pone.0073614.
[94] S.M. Ullrich, T.W. Tanton, S.A. Abdrashitova, Mercury in the aquatic environment: a review of factors affecting methylation, Crit. Rev. Environ. Sci. Technol. 31 (3) (2001) 241–293.
[95] R.D.S. Raposo, D.V. Pinto, R. Moreira, R.P. Dias, C.A. Fontes Ribeiro, R.B. Oriá, J. O. Malva, Methylmercury impact on adult neurogenesis: is the worst yet to come from recent brazilian environmental disasters? Front Aging Neurosci. 12 (2020), 591601 https://doi.org/10.3389/fnagi.2020.591601. PMID: 33328968; PMCID: PMC7719787.
[96] M. Farina, K.C. Dahm, F.D. Schwalm, A.M. Brusque, M.E. Frizzo, G. Zeni, et al., Methylmercury increases glutamate release from brain synaptosomes and glutamate uptake by cortical slices from suckling rat pups: modulatory effect of ebselen, Toxicol. Sci. 73 (1) (2003) 135–140, https://doi.org/10.1093/toxsci/kfg058.
[97] J.K. Fahrion, Y. Komuro, Y. Li, N. Ohno, Y. Littner, E. Raoult, L. Galas, D. Vaudry, H. Komuro, Rescue of neuronal migration deficits in a mouse model of fetal Minamata disease by increasing neuronal Ca2+ spike frequency, Proc. Natl. Acad. Sci. USA 109 (13) (2012) 5057–5062, https://doi.org/10.1073/pnas.1120747109 (PMID: 22411806; PMCID: PMC3323999).

[98] K.K. Aminzadeh, M. Etminan, Dental amalgam and multiple sclerosis: a systematic review and meta-analysis, J. Public Health Dent. 67 (1) (2007) 64–66, https://doi.org/10.1111/j.1752-7325.2007.00011.x.

[99] J. Mutter, A. Curth, J. Naumann, R. Deth, H. Walach, Does inorganic mercury play a role in Alzheimer's disease? A systematic review and an integrated molecular mechanism, J. Alzheimers Dis. 22 (2) (2010) 357–374, https://doi.org/10.3233/JAD-2010-100705.

[100] A.E. Abdel Moneim, The neuroprotective effect of berberine in mercury-induced neurotoxicity in rats, Metab. Brain Dis. 30 (4) (2015) 935–942, https://doi.org/10.1007/s11011-015-9652-6. Epub 2015 Jan 21.

[101] F.O. Johnson, Y. Yuan, R.K. Hajela, A. Chitrakar, D.M. Parsell, W.D. Atchison, Exposure to an environmental neurotoxicant hastens the onset of amyotrophic lateral sclerosis-like phenotype in human Cu2+/Zn2+ superoxide dismutase 1 G93A mice: glutamate-mediated excitotoxicity, J. Pharm. Exp. Ther. 338 (2) (2011) 518–527, https://doi.org/10.1124/jpet.110.174466. Epub 2011 May 17. PMID: 21586603; PMCID: PMC3141904.

[102] M.L. Seibenhener, M.C. Wooten, Use of the open field maze to measure locomotor and anxiety-like behavior in mice, J. Vis. Exp. (96) (2015), e52434, https://doi.org/10.3791/52434. PMID: 25742564; PMCID: PMC4354627.

[103] A.K. Kraeuter, P.C. Guest, Z. Sarnyai, The open field test for measuring locomotor activity and anxiety-like behavior, Methods Mol. Biol. 1916 (2019) 99–103, https://doi.org/10.1007/978-1-4939-8994-2_9.

[104] H. Takeshita, K. Yamamoto, S. Nozato, T. Inagaki, H. Tsuchimochi, M. Shirai, R. Yamamoto, Y. Imaizumi, K. Hongyo, S. Yokoyama, M. Takeda, R. Oguro, Y. Takami, N. Itoh, Y. Takeya, K. Sugimoto, S.I. Fukada, H. Rakugi, Modified forelimb grip strength test detects aging-associated physiological decline in skeletal muscle function in male mice, Sci. Rep. 7 (2017) 42323, https://doi.org/10.1038/srep42323. PMID: 28176863; PMCID: PMC5296723.

[105] R.W. Bohannon, S.R. Magasi, D.J. Bubela, Y.C. Wang, R.C. Gershon, Grip and knee extension muscle strength reflect a common construct among adults, Muscle Nerve 46 (4) (2012) 555–558, https://doi.org/10.1002/mus.23350. PMID: 22987697; PMCID: PMC3448119.

[106] R.W. Bohannon, Grip strength: an indispensable biomarker for older adults, Clin. Inter. Aging 14 (2019) 1681–1691, https://doi.org/10.2147/CIA.S194543. PMID: 31631989; PMCID: PMC6778477.

[107] A. Can, D.T. Dao, M. Arad, C.E. Terrillion, S.C. Piantadosi, T.D. Gould, The mouse forced swim test, J. Vis. Exp. (59) (2012), e3638, 10.3791/3638. PMID: 22314943; PMCID: PMC3353513.

[108] M. Chatterjee, M. Jaiswal, G. Palit, Comparative evaluation of forced swim test and tail suspension test as models of negative symptom of schizophrenia in rodents, ISRN Psychiatry 2012 (2012), 595141, https://doi.org/10.5402/2012/595141. PMID: 23738205; PMCID: PMC3658575.

[109] R. Yankelevitch-Yahav, M. Franko, A. Huly, R. Doron, The forced swim test as a model of depressive-like behavior, J. Vis. Exp. 97 (2015), 52587, https://doi.org/10.3791/52587. PMID: 25867960; PMCID: PMC4401172.

[110] C.D. Barnhart, D. Yang, P.J. Lein, Using the Morris water maze to assess spatial learning and memory in weanling mice, PLOS One 10 (4) (2015), e0124521, https://doi.org/10.1371/journal.pone.0124521. PMID: 25886563; PMCID: PMC4401674.

[111] C.V. Vorhees, M.T. Williams, Morris water maze: procedures for assessing spatial and related forms of learning and memory, Nat. Protoc. 1 (2) (2006) 848–858, https://doi.org/10.1038/nprot.2006.116. PMID: 17406317; PMCID: PMC2895266.

[112] D. Albores-Garcia, L.C. Acosta-Saavedra, A.J. Hernandez, M.J. Loera, E. S. Calderón-Aranda, Early developmental low-dose methylmercury exposure alters learning and memory in periadolescent but not young adult rats, Biomed. Res. Int. 2016 (2016), 6532108, https://doi.org/10.1155/2016/6532108. Epub 2016 Jan 13. PMID: 26885512; PMCID: PMC4738696.

[113] L. Colucci-D'Amato, C. Perrone-Capano, U. di Porzio, Chronic activation of ERK and neurodegenerative diseases, Bioessays 25 (11) (2003) 1085–1095, https://doi.org/10.1002/bies.10355.

[114] S. Mahmoud, M. Gharagozloo, C. Simard, D. Gris, Astrocytes maintain glutamate homeostasis in the CNS by controlling the balance between glutamate uptake and release, Cells 8 (2) (2019) 184, https://doi.org/10.3390/cells8020184. PMID: 30791579; PMCID: PMC6406900.

[115] T. Filipi, Z. Hermanova, J. Tureckova, O. Vanatko, A.M. Anderova, Glial cells-the strategic targets in amyotrophic lateral sclerosis treatment, J. Clin. Med. 9 (1) (2020) 261, https://doi.org/10.3390/jcm9010261. PMID: 31963681; PMCID: PMC7020059.

[116] N.R. Carlson, Physiology of behavior, Pearson High. Ed. 2 (2016).

[117] C. Lappe-Siefke, S. Goebbels, M. Gravel, E. Nicksch, J. Lee, P.E. Braun, I. R. Griffiths, K.A. Nave, Disruption of Cnp1 uncouples oligodendroglial functions in axonal support and myelination, Nat. Genet 33 (3) (2003) 366–374, https://doi.org/10.1038/ng1095. Epub 2003 Feb 18.

[118] K. Kingwell, Amyotrophic lateral sclerosis: early involvement of grey matter oligodendrocytes in amyotrophic lateral sclerosis, Nat. Rev. Neurol. 9 (5) (2013) 238, https://doi.org/10.1038/nrneurol.2013.78. Epub 2013 Apr 23.

[119] S.H. Kang, Y. Li, M. Fukaya, I. Lorenzini, D.W. Cleveland, L.W. Ostrow, J. D. Rothstein, D.E. Bergles, Degeneration and impaired regeneration of gray matter oligodendrocytes in amyotrophic lateral sclerosis, Nat. Neurosci. 16 (5) (2013) 571–579, https://doi.org/10.1038/nn.3357. Epub 2013 Mar 31. PMID: 23542689; PMCID: PMC3637847.

[120] N.K. Iwata, J.Y. Kwan, L.E. Danielian, J.A. Butman, F. Tovar-Moll, E. Bayat, M. K. Floeter, White matter alterations differ in primary lateral sclerosis and amyotrophic lateral sclerosis, Brain 134 (Pt 9) (2011) 2642–2655, doi: 10.1093/brain/awr178. Epub 2011 Jul 28. PMID: 21798965; PMCID: PMC3170531.

[121] C. Schuster, M. Elamin, O. Hardiman, P. Bede, The segmental diffusivity profile of amyotrophic lateral sclerosis associated white matter degeneration, Eur. J. Neurol. 23 (8) (2016) 1361–1371, https://doi.org/10.1111/ene.13038. Epub 2016 May 21.

[122] T. Philips, A. Bento-Abreu, A. Nonneman, W. Haeck, K. Staats, V. Geelen, N. Hersmus, B. Küsters, L. Van Den Bosch, P. Van Damme, W.D. Richardson, W. Robberecht, Oligodendrocyte dysfunction in the pathogenesis of amyotrophic lateral sclerosis, Brain 136 (Pt 2) (2013) 471–482, https://doi.org/10.1093/brain/aws339. Epub 2013 Jan 31. PMID: 23378219; PMCID: PMC3572934.

[123] J. Lasiene, K. Yamanaka, Glial cells in amyotrophic lateral sclerosis, Neurol. Res. Int. 2011 (2011), 718987, 10.1155/2011/718987. Epub 2011 Jun 7. PMID: 21766027; PMCID: PMC3135155.

[124] S. Maniatis, T. Äijö, S. Vickovic, C. Braine, K. Kang, A. Mollbrink, D. Fagegaltier, Ž. Andrusivová, S. Saarenpää, G. Saiz-Castro, M. Cuevas, A. Watters, J. Lundeberg, R. Bonneau, H. Phatnani, Spatiotemporal dynamics of molecular pathology in amyotrophic lateral sclerosis, Science 364 (6435) (2019) 89–93, https://doi.org/10.1126/science.aav9776.

[125] B. Favaloro, N. Allocati, V. Graziano, C. Di Ilio, V. De Laurenzi, Role of apoptosis in disease, Aging 4 (5) (2012) 330–349, https://doi.org/10.18632/aging.100459. PMID: 22683550; PMCID: PMC3384434.

[126] I. Sen, A. Nalini, N.B. Joshi, P.G. Joshi, Cerebrospinal fluid from amyotrophic lateral sclerosis patients preferentially elevates intracellular calcium and toxicity in motor neurons via AMPA/kainate receptor, J. Neurol. Sci. 235 (1–2) (2005) 45–54, https://doi.org/10.1016/j.jns.2005.03.049.

[127] E. Foran, D. Trotti, Glutamate transporters and the excitotoxic path to motor neuron degeneration in amyotrophic lateral sclerosis, Antioxid. Redox Signal 11 (7) (2009) 1587–1602, https://doi.org/10.1089/ars.2009.2444. PMID: 19413484; PMCID: PMC2842587.

[128] M.S. Uddin, A. Al Mamun, M.T. Kabir, M. Nasrullah, F. Wahid, M.M. Begum, Z. K. Labu, M.S. Rahman, M.T. Islam, M.S. Amran, M.M. Abdel-Daim, Neurochemistry of neurochemicals: messengers of brain functions, J. Intellect. Disabil. Diagn. Treat. 5 (4) (2018) 137–151.

[129] L. Köles, E. Kató, A. Hanuska, Z.S. Zádori, M. Al-Khrasani, T. Zelles, P. Rubini, P. Illes, Modulation of excitatory neurotransmission by neuronal/glial signalling molecules: interplay between purinergic and glutamatergic systems, Purinergic Signal. 12 (1) (2016) 1–24, https://doi.org/10.1007/s11302-015-9480-5. Epub 2015 Nov 6. PMID: 26542977; PMCID: PMC4749532.

[130] B.R. Foerster, M.G. Pomper, B.C. Callaghan, M. Petrou, R.A. Edden, M. A. Mohamed, R.C. Welsh, R.C. Carlos, P.B. Barker, E.L. Feldman, An imbalance between excitatory and inhibitory neurotransmitters in amyotrophic lateral sclerosis revealed by use of 3-T proton magnetic resonance spectroscopy, JAMA Neurol. 70 (8) (2013) 1009–1016, https://doi.org/10.1001/jamaneurol.2013.234. PMID: 23797905; PMCID: PMC4382938.

[131] J. Lewerenz, P. Maher, Chronic glutamate toxicity in neurodegenerative diseases – what is the evidence? Front. Neurosci. 9 (2015), 469 https://doi.org/10.3389/fnins.2015.00469.

[132] B.G. Park, C.I. Yoo, H.T. Kim, C.H. Kwon, Y.K. Kim, Role of mitogen-activated protein kinases in hydrogen peroxide-induced cell death in osteoblastic cells, Toxicology 215 (1–2) (2005) 115–125, https://doi.org/10.1016/j.tox.2005.07.003.

[133] Y.J. Jung, D. Tweedie, M.T. Scerba, N.H. Greig, Neuroinflammation as a factor of neurodegenerative disease: thalidomide analogs as treatments, Front. Cell Dev. Biol. 7 (2019) 313, https://doi.org/10.3389/fcell.2019.00313. PMID: 31867326; PMCID: PMC6904283.

[134] J.A. Smith, A. Das, S.K. Ray, N.L. Banik, Role of pro-inflammatory cytokines released from microglia in neurodegenerative diseases, Brain Res. Bull. 87 (1) (2012) 10–20, https://doi.org/10.1016/j.brainresbull.2011.10.004. Epub 2011 Oct 18.

[135] L.* Singh, S. Rana, S. Mehan, Role of adenylyl cyclase activator in controlling experimental diabetic nephropathy in rats, Int. J. Physiol. Pathophysiol. Pharmacol. 10 (5) (2018) 144–153. PMID: 30515257; PMCID: PMC6261921.

[136] Z. Yin, D. Milatovic, J.L. Aschner, T. Syversen, J.B. Rocha, D.O. Souza, M. Sidoryk, J. Albrecht, M. Aschner, Methylmercury induces oxidative injury, alterations in permeability and glutamine transport in cultured astrocytes, Brain Res. 1131 (1) (2007) 1–10, https://doi.org/10.1016/j.brainres.2006.10.070. Epub 2006 Dec 19. PMID: 17182013; PMCID: PMC1847599.

[137] V. Glaser, E.M. Nazari, Y.M. Müller, L. Feksa, C.M. Wannmacher, J.B. Rocha, A. F. De Bem, M. Farina, A. Latini, Effects of inorganic selenium administration in methylmercury-induced neurotoxicity in mouse cerebral cortex, Int. J. Dev. Neurosci. 28 (7) (2010) 631–637.

[138] J. Pedraza-Chaverrí, L.M. Reyes-Fermín, E.G. Nolasco-Amaya, M. Orozco-Ibarra, O.N. Medina-Campos, O. González-Cuahutencos, I. Rivero-Cruz, R. Mata, ROS scavenging capacity and neuroprotective effect of alpha-mangostin against 3-nitropropionic acid in cerebellar granule neurons, Exp. Toxicol. Pathol. 61 (5) (2009) 491–501, https://doi.org/10.1016/j.etp.2008.11.002. Epub 2008 Dec 23.

[139] M.P. Phyu, J. Tangpong, Neuroprotective effects of xanthone derivative of Garcinia mangostana against lead-induced acetylcholinesterase dysfunction and cognitive impairment, Food Chem. Toxicol. 70 (2014) 151–156, https://doi.org/10.1016/j.fct.2014.04.035. Epub 2014 Apr 30.

[140] L. Ferraiuolo, K. Meyer, T.W. Sherwood, J. Vick, S. Likhite, A. Frakes, C. J. Miranda, L. Braun, P.R. Heath, R. Pineda, C.E. Beattie, Oligodendrocytes contribute to motor neuron death in ALS via SOD1-dependent mechanism, Proc. Natl. Acad. Sci. USA 113 (42) (2016) E6496–E6505.

[141] A. Nonneman, W. Robberecht, Den, L.V. Bosch, The role of oligodendroglial dysfunction in amyotrophic lateral sclerosis, Neurodegener. Dis. Manag. 4 (3) (2014) 223–239.

[142] S.H. Vaz, S. Pinto, A.M. Sebastião, D. Brites, Astrocytes in Amyotrophic Lateral Sclerosis, Exon Publications, 2021, pp. 35–53.
[143] M.R. Vargas, J.A. Johnson, Astrogliosis in amyotrophic lateral sclerosis: role and therapeutic potential of astrocytes, Neurotherapeutics 7 (4) (2010) 471–481.
[144] J. Brettschneider, J.B. Toledo, V.M. Van Deerlin, L. Elman, L. McCluskey, V. M. Lee, J.Q. Trojanowski, Microglial activation correlates with disease progression and upper motor neuron clinical symptoms in amyotrophic lateral sclerosis, PLOS One 7 (6) (2012), e39216.
[145] E.Mehmood Siddiqui, S. Mehan, S. Upadhayay, A. Khan, M. Halawi, A. Ahmed Halawi, R.M. Alsaffar, Neuroprotective efficacy of 4-Hydroxyisoleucine in experimentally induced intracerebral hemorrhage, Saudi J. Biological Sci. 28 (11) (2021) 6417–6431, https://doi.org/10.1016/j.sjbs.2021.07.010.